DIAGNOSTICS OF LOW PRESSURE GAS DISCHARGES

S. B/

NUCLEAR ENGINEERING AND TECHNOLOGY PROGRAMME
INDIAN INSTITUTE OF TECHNOLOGY, KANPUR
AUGUST 1984

DIAGNOSTICS OF LOW PRESSURE GAS DISCHARGES

A thesis submitted
in Partial Fulfilment of the Requirements
for the degree of

MASTER OF TECHNOLOGY

by
S. BALARAMAN

to the

NUCLEAR ENGINEERING AND TECHNOLOGY PROGRAMME
INDIAN INSTITUTE OF TECHNOLOGY, KANPUR
AUGUST 1984

TO

MY LOVING PARENTS

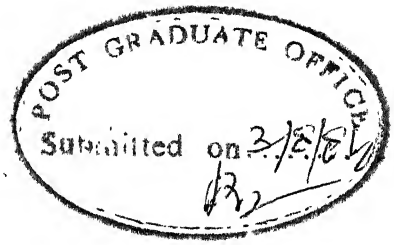

CERTIFICATE

This is to certify that the work DIAGNOSTICS OF LOW PRESSURE GAS DISCHARGES has been carried out under my supervision and that this has not been submitted elsewhere for a degree.

A. R. DAS
Professor and Head
Nuclear Engineering and
Technology Programme
Indian Institute of Technology
Kanpur 208016 , India

August 1984.

7/8/84

ACKNOWLEDGEMENTS

I am grateful to Prof. K. Sri Ram for suggesting me the problem and helping me bring up the plasma laboratory in the initial stages. In the later stages, Prof. A.R. Das recognized various difficulties that were cropping up with the experiments, and gave me constant encouragement. I express my profound thanks to him.

I would also like to thank Dr. K. Jothimurugesan for supplying me gases required and many other components that were needed from time to time.

I wish to thank Mr. R. Venugopal for his assistance during designing and experimentation. My thanks are also due to Mr. Patak and Mr. Tripati for their technical help.

S. Balaraman

ABSTRACT

In the first part of the experiments, the effect of transverse magnetic field on breakdown potentials for air, argon, CO_2, hydrogen, nitrogen, and oxygen is studied. The equivalent-pressure-concept, that is the application of transverse magnetic field is equivalent to the increase of pressure of the gas, is briefly discussed. Using this concept and from the Paschen curves the electron-molecule collision frequency is determined for these gases. It is found that the collision frequencies deduced from the breakdown voltage data of low magnetic fields differ from those of medium and relatively higher magnetic fields. It is also found that the collision frequencies from high magnetic field data are close to those reported earlier. The variation of discharge current with magnetic field is also studied.

In the second part, a Langmuir probe of tungsten wire with translatory mechanism is fabricated. This probe is used to measure the electron density and temperature in the positive column of glow discharge in air, argon, CO_2, nitrogen, and oxygen. It is found that the experimental temperature values are in close agreement with the theoretical values, whereas the density values are lower than the theoretical values.

CONTENTS

LIST OF FIGURES

LIST OF TABLES

CHAPTER 1

INTRODUCTION

1.1 BACKGROUND

The study of the conduction of electricity through a gas was one of the oldest phenomena in physics which started as early as 19th century. Electrical discharge is one of the ways to induce ionization and hence plasma - a state of charged particles in quasi-neutrality - in gases. It appears that discharge physics started in England (1) and so it is less surprising that workers like I. Langmuir - Father of Plasma Physics - J.J. Thomson , F.W. Aston, W.P. Allis, F.L. Jones, G. Francis - other founding fathers - were all from Great Britain.

Though search for such a state of matter as plasma was made earlier, it was in 1800 when Davy in England and Petroff in Russia (1) discovered the arc discharge. Since then, the discharge physics has come a long way projecting a wide spectrum. Between the years 1831 and 1835 Faraday (1), working at the Royal Institution, discovered glow discharge. It really got an impetus after the discovery of cathode rays (electrons) in 1895 by Perrin and canal rays (positive ions) in 1886 by Goldstein in electrical discharges. Later investigations by J.J. Thomson and Aston, and particularly Wien furnished valuable data about the

properties of beams of electrons and positive ions - a field which is by no means yet exhausted. The complexity of true analysis is obvious as there are some 110 processes taking place, as listed by Hasted (2), in an ionized gas Analyses have been carried out and theories developed by Loeb (3,4), von Engel (5,1), Allis (6), Francis (7), and many others for prominent phenomena, and explained through rate coefficients and collision data.

The quantitative study of discharges in transverse and longitudinal magnetic fields was started in 1930's. The theory of electron drift in magnetic field has been developed by Tonks and Allis (8), and the experimentation of longitudinal magnetic field was first done by Cummings et al. (9). The first experimental work on the influence of a homogeneous transverse magnetic field was carried out by Beckman (10) who studied studied axial field strength and electron energy distribution. The influence of a crossed magnetic field on Townsend discharge has has been studied by Heylen(11). When a crossed magnetic field is applied to a gaseous Townsend discharge, the charged particles are deflected into cycloidal paths. This increases the probability of a collision and hence causes a reduction in the electron mean-free-path. This can be interpreted as an apparent increase in pressure. This equivalent pressure concept, first developed by Townsend and Gill (12) and Blevin and Haydon (13), was later tried in different situations and

substantiated by Dargan and Heylen (14), Haydon (15), Guharay and Sen Gupta (16), and lately by Sen Gupta et al. (17).

The oldest diagnostic technique in a plasma is electrostatic probe - also known as Langmuir probe - the theory and application of which were first developed by Langmuir and Mott-Smith (18). Though there are other accurate diagnostic methods developed now, Langmuir probe still finds wide application in a plasma laboratory.

1.2 OUTLINE OF THE PRESENT WORK

The basic study in plasma science would involve the account of ionization, particle collisions, transport properties of the constituents, decay processes etc. on a microscopic scale. A macroscopic view would consider a group of particles of high density as fluid, and analyse it by using familiar fluid mechanics equations.

The purpose of this work is to develop a simple plasma laboratory and the associated diagnostic techniques. In the present effort, discharge tubes are designed, including a vacuum system, making electrical circuitry, and the fabricatio of a Langmuir probe. The present work centers around an experimental investigation of two different features of electr cal discharge. In the first, electrical breakdown of gases in a magnetic field, transverse to the electric field direction in the discharge tube, is studied. Using equivalent pressure

concept, electron-molecule collision frequency is determined from the breakdown potential data. This study is done in air, N_2,H_2,O_2,A, and CO_2 with magnetic fields in the range of 0 to 3000 Gs (0 - 0.3 Tesla). The variation of the discharge current in magnetic field is also studied.

In the second part of the study, Langmuir probe diagnostics of the positive column in a glow discharge is carried out. A probe of tungsten wire with translation mechanism is fabricated and made use of in determining the electron temperature and electron density. Diagnostics of the positive column is carried out in air, N_2, O_2, A, and CO_2. Electron temperature and number density are determined for various discharge currents at two radial positions. The experimental results are compared with theoretical estimates. Chapters 2 and 3 summarize electrical discharge phenomena and glow discharge characteristics.

CHAPTER 2

ELECTRICAL BREAKDOWN OF GASES

2.1 INTRODUCTION

The low pressure gas discharge is one of the most well known phenomena in physics, and has been closely studied for more than a century. Although considerable work had been done earlier on gaseous discharges, particularly at high pressures, Langmuir's research was on low-pressure discharges and his papers written in collaboration with H. Mott-Smith (18) are considered classics in the field. But it seems it is Faraday in 1831, working at the Royal Institution, who discovered that the current could pass through a discharge tube filled with a gas at low pressure without showing any luminosity at all, which he called a dark discharge. Low-pressure refers to the pressure range of 10^{-2} torr to 10 torr with no sharp boundary with vacuum or high-pressure region.

2.2 ELECTRICAL BREAKDOWN OF GASES

The electrical breakdown of gas is a phenomenon which is observed when a gas or vapour becomes electrically conducting. Under these conditions free electric charges are present and can move through the gas, usually under the influence of an electric field: the gas is said to be ionized. When we speak

of an ionized gas, we imply that through some mechanism we have separated one or more electrons from some of the atoms or molecules, resulting in a gaseous medium containing electrons, ions and neutral atoms or molecules. A weakly ionized gas would have one atom or molecule ionized in 10^6, or more, neutrals. A fully ionized gas would consist entirely of charged particles whose behaviour is quite different from that of weakly ionized gases. Plasma is an ionized gas which is quasi-neutral and whose characteristic dimension is much smaller than the dimensions of the container.

The problem of complete gaseous breakdown can well be considered in two aspects: first, the elucidation of mechanism which sets the criterion that must be satisfied before breakdown is at all possible; and secondly, the mechanism by which an ionization current can increase, when once breakdown criterion is satisfied, to produce first a glow discharge and then the glow-to-arc transition. The first aspect is discussed here, and the second will be taken up towards the end of this chapter.

Let us consider an experimental apparatus consisting of two plane, parallel, metallic electrodes separated by a distance, enclosing a gas of a few torr pressure and connected to a D.C. potential source. When the voltage across the electrodes is raised very slowly and the current is observed with a very

sensitive instrument, random current pulses of less than 10^{-14} A/cm^2 magnitude will be the first measurable current. However, when enough free electrons are present in the gap, as a consequence of external volume ionization, a steady current may be observed. External sources such as UV illumination of the cathode and cosmic rays may be used to produce electrons and ions, and the passage of photoelectric current, under a constant radiation level, will increase with the voltage until it reaches a plateau known as the saturation current. At this stage a non-self-sustaining discharge is said to have been established, because once the external sources are removed the steady-state current will cease to flow.

Increasing the voltage across the gap will not affect the current, I, for some time (see Fig. 1) but beyond a certain voltage, I will start to increase again. This increase is exponential and this region is called the Townsend discharge. Further increase of the voltage will lead to an over-exponential increase in the current followed by a collapse of the voltage across the gap. This abrupt transition is known as breakdown and the gas which behaved as an insulator earlier has become electrically conducting. The current now is self-sustained and external sources become unnecessary to set the current flowing. But in practice, no UV illumination of cathode is necessary. Ionization due to natural radioactivity or cosmic rays provides initiatory electrons. If the potential V_s at

which the breakdown occurs is called the breakdown or sparking potential. If the current is allowed to increase further by cutting down the series resistance of the outer circuit or by supplying more voltage to the plates, the voltage across the discharge will begin to drop until it reaches a low level and enter into different discharge regimes as shown in Fig. 1. Once the breakdown current in a gas has begun to rise rapidly to significant magnitude, it is clear that the potential across the electrodes must depend upon the characteristic of the external circuit. If the discharge tube is connected to a DC supply without any resistance in series, provided the voltage is sufficient to start the discharge, the current will certainly grow until some part of the circuit breaks down.

Explanation of the increase of current density beyond its saturation value rests on the ionization of the gas by the primary electrons, that is the initiatory electrons and the resultant increase in electron population produced by the chain-like collisions. The primary collision produce fresh ions and electrons that eventually lead to the establishment of a discharge mechanism. Electrons produced by the external ionizing agent (radiation, cosmic ray) can acquire an energy from the electric field which is sufficient for them in turn to ionize the molecules of the gas. The same will be true for the secondary electrons and this chain would

repeat itself. This avalanche effect produces a rapid increase in the current in the discharge tube.

Ionization in a gas is due to different types of collisions among various constituents. Different collision processes have been dealt with in detail by Hasted (2). Ionization and excitation by electrons in an electric field has been treated by von Engel (1). In gaseous discharges, the ionization and non-ionization processes can be classified as gaseous processes and cathode processes. For details of these processes one can refer to Meek and Craggs (19).

2.3 SPARKING CRITERION AND PASCHEN'S LAW

2.3.1 Sparking Criterion

Let's consider our system with electrodes separated by a distance d, which is greater than a few electronic mean free paths. We can define a macroscopic coefficient α, which represents the mean number of ion pairs formed by an electron in a path of 1 cm. A cathode electron produces αd ionizing collisions along d. Thus the increase in the number of ion pairs along the element of length dx is αdx per electron, and for N_x electrons at x we obtain

$$dN = N_x \alpha dx \qquad (2.1)$$

By integrating between x = o and x = d we obtain for the number of electrons N at d or the current i which is proportional to N at d

$$\frac{N}{N_o} = \frac{i}{i_o} = e^{\alpha d} \qquad (2.2)$$

where N_o is the number of electrons per cm^3 and i_o the current produced by irradiation of the cathode. The coefficient α is often called Townsend's first ionization coefficient and its value depends on the field E, the pressure p, and the type of gas. For each electron starting from the cathode and for $e^{\alpha d}$ electrons reaching the anode, simultaneously $e^{\alpha d}-1$ positive ions arrive at the cathode; the difference is due to the fact that the first electron liberated at the cathode was taken to be unaccompanied by a positive ion. According to Eqn. (2.2) the electrons liberated at the cathode are multiplied by ionizing collisions in an electric field. The current i depends on the magnitude of radiation incident on the cathode. If the radiation is cut-off, N_o and i_o will be zero and so will be i. In some cases, especially under low pressure, the primary electrons cannot ionize in the vicinity of the cathode because of their low kinetic energy. Only when they have acquired enough KE to equal the ionization energy V_i does the Eqn. (2.2) become valid. The distance ∂ from the cathode, in which no ionization takes place is given by

$$\partial = \frac{V_i}{E}$$

At high fields ∂ is therefore negligible but at low fields, or low pressure, it is appreciable and must be taken into account in Eqn. (2.2), which becomes

$$i = i_o \, e^{\alpha(x-\partial)} \qquad (2.3)$$

By measuring i and i_o as function of position x, α can be determined.

The cause of over-exponential increase in current after saturation current (Fig. 1) can be sought in various processes which take place either within the gas or at the cathode. In the gas the positive ions can ionize further atoms by collision. These gas processes are termed β-processes, β being Townsend's second coefficient of ionization. At the cathode, the ions, by means of their potential and kinetic energy, liberate secondary electrons. Cathode process are usually referred to as secondary or γ-processes. Photoelectric emission is denoted by the coefficient ∂ and cathode emission due to incidence of excited atoms ε. Normally, γ-processes dominate in the breakdown mechanism. With the secondary processes taken into account, the number of electrons arriving at the anode per unit area per sec can be derived as

$$N = N_o \frac{e^{\alpha d}}{1-\gamma(e^{\alpha d}-1)} \qquad (2.4)$$

Or

$$\frac{i}{i_o} = \frac{e^{\alpha d}}{1-\gamma(e^{\alpha d}-1)} \qquad (2.5)$$

From this expression it is seen that for an avalanche (or breakdown) to take place the denomenator should be equal to zero. That is

$$1 - \gamma(e^{\alpha d}-1) = 0 \qquad (2.6)$$

when the condition (2.6) is satisfied breakdown occurs, and it means that the current in a discharge becomes unstable and thus a large current may develop without a foreign agency liberating electrons at the cathode; the original discharge goes over into a self-sustaining discharge. Equation (2.6) is the sparking or breakdown criterion. Ionization, cathode processes and self-sustaining discharge are thoroughly treated by von Engel (1), Nasser (20) and Meek and Craggs (19). It is advantageous to use reduced parameters like E/p, α/p, pd, etc., since it shows at once whether a particular relation obeys the rule of similarity or not.

Primary ionization, α, depends on the gas, pressure, and the field. For a particular gas α/p varies with E/p according to

$$\alpha/p = A\, e^{-Bp/E} \qquad (2.7)$$

where A and B are gas constants, subject to a range of E/p.

2.3.2 Paschen's law

If a slowly increasing potential difference is applied across the plane parallel electrodes, separated by a distance d, it is well known that at some critically defined potential difference, V_s, electrical breakdown of the gas at pressure p, occurs. Experiments have shown that V_s varies according to the similarity relationship

$$V_s = f(pd)_s \qquad (2.8)$$

where f represents some function of $(pd)_s$ which is the value of pd at which a spark occurs.

The relationship is known as Paschen's law.

V_s vs $(pd)_s$ curve is called Paschen curve. The general shape of Paschen curve is as shown in one of the experimental V_s-pd curves (Fig. 8). The nature of the curves is explained as follows : at very low pressures the collision frequency is low, so that sufficient ionization is maintained only by increasing the probability of ionization at each collision; consequently, the electron velocity, and thus the electric field, must be high. Hence V_s must increase as p diminishes when p is very low (left of the minimum). On the other hand at higher pressures the collision frequency is high, and the rate of energy loss is correspondingly high, while the energy gained

per free path is low unless the field is correspondingly high. Thus for a fixed electrode sepreation distance, E_s ($= V_s/ds$) must be increased when p is increased at the high pressures (right of the minimum); and the curve shows a minimum. Paschen's law applies to the condition where E is uniform while pd is varying. The law helps to arrive at an expression for breakdown potential :

$$V_s = \frac{Bpd}{\ln\left[\frac{Apd}{\ln(1+\frac{1}{\gamma})}\right]} \quad \text{and} \qquad (2.9)$$

V_s minimum is given as

$$(V_s)_{min} = 2.718 \frac{B}{A} \ln(\frac{1}{\gamma} + 1) \qquad (2.10)$$

obtained by differentiating (2.14) with respect to pd and equating the derivative to zero.

At extremely high and low values of pd, deviation from the law has been observed in which V_s ceases to be a unique function of pd but rather varies with p when pd is held constant. At larger values of pd 'streamer' mechanism will become responsible for the breakdown, and the Townsend mechanism ceases to be active. At very low pressures, gaseous processes become less significant and the breakdown is usually initiated from the electrodes (vacuum breakdown).

Furthermore the law is not applicable in many gaseous mixtures, especially in Penning mixtures, where the admixture can be ionized directly by the metastables of the main gas. In this discussion, the assumption is that γ is not a function of E/p but is constant. In reality, γ is not only a function of E/p but also of p. This also leads to deviations from the Paschen law. Although in many nonuniform field configurations the law was found to hold both in theory and experiment, yet its applicability is usually limited to very small ranges of pd, as measurements in point-to-plane geometry have shown. In electronegative gases, the Paschen law holds in general and specifically within a limited range around breakdown minimum. α for different gases at different electric fields are given by Loeb (4).

2.3.3 Characterization of a Discharge

Applying an electric field to a gas at low pressure, one observes a number of interesting discharge regimes when the current density is slowly increased. This is illustrated in Fig. 1. It is the current density rather than the current which determines the properties of the discharge. The species involved in a gaseous discharge or an ionized gas are neutrals, charged particles (negative and positive ions, and electrons), and excited atoms/molecules and photon. In an un-ionized gas, the gas number density at 1 torr and $0^{o}C$, is typically

3.54×10^{22} m^{-3} . For typical gas discharges the electron densities are expected to lie in the range of 10^{16} to 10^{20} m^{-3}. We will have positive ions, naturally, and negative ions as well. Though ion species also affect the electrical properties of the discharge, it is the electrons that usually dominate. We will be also interested in what is known as quasi-neutrality, where strong electrostatic fields are not present. This implies that the net charge density is approximately zero. Optical properties of a discharge are due to excited atoms/molecules and photons. They are of prime importance for lasers, light sources or other devices where quantum effects occur. The real basis of the study of gas discharges involves the interaction between these species. Some of the important interactions are summarized in Appendix.

2.4 BASIC CHARACTERIZATION OF ELECTRONS

Electron is the species which is usually of overwhelming importance in determining the electrical and optical properties of a discharge. One of the most significant characterizations of a gas discharge is given by the electron number density, n_e, and the electron temperature T_e, or the energy of the electrons. The density n_e for glows is between 10^{15} m^{-3} and 10^{20} m^{-3} and that for arcs is above 10^{20} m^{-3} upto, say, 10^{25} m^{-3}. The temperature for both the cases is between 10^3K and 5×10^5 K.

Electron density parameter is straightforward and in most gas discharges it is linearly related to the electric current through the medium. Electron temperature parameter is a consequence of the 'statistical' nature of the electron gas. In thermodynamic equilibrium, the distribution of electron velocities (or energies) is given by the Maxwellian distribution which allows the electron temperature, T_e, to be defined by :

$$\frac{m\langle v^2\rangle}{2} = \frac{3kT_e}{2} \qquad (2.11)$$

where $\langle v^2\rangle$ is mean square velocity

k Boltzmann's constant

m the electron mass, and

T_e the electron temperature

A moderate electric field being assumed, the electrons moving in a gas be treated as a swarm of particles which have both a random and a drift velocity. The random velocity of the electron swarm - equivalent to the mean energy or electron temperature - is the velocity at or near the peak of the distribution curve, whereas the drift velocity is the average velocity with which the centre of the swarm moves in field direction. These two velocities are of different order of magnitude - the drift velocity is often less than 10^{-3} of the random velocity. It is only because of the distribution of

random velocities that there are electrons which have energies above that necessary for ionization. The motion of electrons and ions is well treated by Allis (6), and drift and diffusion by Huxley and Crompton (21), and by Hasted (2).

The electron swarm in a field can be regarded as a hot electron gas which is mixed with the colder gas. This concept of a gas mixture can lead one to ask why these two components do not exchange readily and so attain a common temperature. The answer is that as long as the average energy acquired by one electron between two collisions is sufficiently large compared with the average energy lost in an encounter, the exchange of energy between the electrons and the neutral gas is small and hence a large temperature can be maintained by the electrons.

Debye length is basically a measure of the distances over which significant deviations from quasi-neutrality are possible. This is a length scale which approximately divides the microscopic domain from the macroscopic domain in a plasma, denoted by λ_D. It can be shown that as long as the distance between two passing particles is appreciably less than λ_D, the normal Coulomb attraction or repulsion will exist and one can define the encounter as a simple collision, to which ordinary laws of particle dynamics apply. However, if the minimum distance of approach of the two particles is greater than λ_D, the collective

motions of the surrounding plasma electrons induced by the passage of the particle will be such as to screen the test particle from the influence of the other particle, or any others beyond the distance λ_D. If ions are considered to be stationary and $n_+ = n_e = n$, then

$$\lambda_D = \left[\frac{kT_e \varepsilon_o}{n_e^2}\right]^{1/2} = 69\sqrt{T_e/n} \quad \text{meters}, \tag{2.12}$$

where T_e is in ^oK and n is in m^{-3}, and ε_o is permittivity constant.

If the dimensions of the ionized medium are comparable to or smaller than λ_D, then wall effects will play an important role on the behavior of the medium. If the dimensions are larger than λ_D, then the moving charges will shield the medium from wall effects. Also, in order for the shielding to be effective, there must be a large number of particles within the Debye sphere, i.e., n_D must be large where

$$n_D = \frac{4}{3} n\pi\lambda_D^3 = 1.38\times10^6 \frac{T_e^{3/2}}{n^{1/2}} \tag{2.13}$$

The Debye length is typically 2.2×10^{-5} m when $n = 10^{18}$ electrons/m^3 and $T_e = 10^5 {}^oK$.

2.4.2 Plasma Frequency

The concept of charge screening indicates that the electrons and ions will adjust their positions to nullify the effect of a charge perturbation. The question is -- how quickly can this occur. This will give an idea of the dynamic behavior of a plasma. Plasma frequency, .. the characteristic frequency of oscillation, defines how quickly an electron moves so an external perturbation can be screened out. Taking a uniform neutral plasma ($n_e = n_+ = n$) and assuming that the ions are stationary, plasma frequency is derived as

$$\omega_p^2 = \frac{ne^2}{m_e \varepsilon_o} = 3.18 \times 10^3 \, n \qquad (2.14)$$

where n is in m^{-3}.

Assuming the motion of an electron under the influence of an electromagnetic field of frequency, ω, the relative dielectric constant of electron gas is given as

$$R = 1 - \frac{n_e^2}{m_e \varepsilon_o \omega^2} = 1 - \frac{\omega_p^2}{\omega^2} \qquad (2.15)$$

Considering the electron gas to be dielectric, if $\omega > \omega_p$, an electromagnetic wave of frequency ω can propagate through the electron gas. If $\omega < \omega_p$, the electromagnetic wave cannot propagate because the relative dielectric constant is negative.

CHAPTER 3

GLOW DISCHARGE

3.1 GENERAL FEATURES

A glow discharge is described as a discharge in which the cathode emits electrons under the bombardment of particles and photons from the gas. The glow discharge derives it name from a luminous zone which develops near the cathode, and has a distinctive arrangement of luminous and dark regions between the cathode and anode, as schematically illustrated in Fig. 2. The actual position of various regions, and indeed the occurrence of a few of them depends upon the pressure and kind of gas, and upon the current. Most regions are, however, common to all.

3.1.1 Glow Regions

Different regions of the glow are shown in Fig. 2.

An increase of pressure causes all negative zones (cathode dark space, negative glow and Faraday dark space) to be compressed towards the cathode. A decrease of pressure causes the reverse effect. If the anode is moved farther apart from the cathode, with a slightly larger voltage, positive column extends to occupy the additional length.

There is no effect on the negative zones as electrodes are moved. When the anode is moved towards the cathode positive column becomes shorter and glow disappears when it moves through Faraday dark space. If the potential and hence the current is increased the length of the cathode dark space decreases, whereas the length of the negative glow increases slightly. Each gas gives a discharge of its characteristic colour. In gases which have low ionization potential the cathode dark space is short. The colour of a certain cathode light, when it appears, depends on the cathode material.

3.1.2 General Mechanism of the Discharge

Electrons emitted from the cathode by the impinging ions have little energy (1 eV) and are rapidly accelerated in a strong field. Within a very short distance they gain energy corresponding to the maximum of the excitation potential, and the cathode layer appears. Spectral lines of lowest energy lie nearest to the cathode, as would be expected. Further from the cathode, though the field has become weaker, the electron ionizes more efficiently and strong electron multiplication will take place. And the electrons so produced are themselves accelerated. Near the boundary between the cathode space and the negative glow the field has become very weak, and thus only the fast electrons which have not lost energy by inelastic collisions will be able to ionize in that

region. However, a large number of electrons will cross the boundary and enter the negative glow.

We have two main groups of electrons entering the negative glow : a large number of slow ones produced by ionization in the cathode dark space, and a fewer fast ones (the primaries) coming straight from the cathode and having almost the full energy of the cathode fall potential. Due to the multiplication the number of electrons able to ionize has increased between the cathode and the glow boundary, and a large number of positive ions has been formed representing a strong positive space charge - this determines the cathode fall. These positive ions will move through the cathode dark space and impinge on the cathode to produce electrons, and so do metastable atoms, fast unexcited atoms, and radiation.

Returning to the electrons of both groups travelling towards anode, their speed is now decreasing with distance. The slow electrons which are easily able to excite but hardly able to ionize produce the intense light which is the cathode end of the glow. The fast electrons dissipate their energy similarly in many inelastic collisions and penetrate further from the cathode, so that the total light intensity in the glow rises to a maximum and then diminishes as we move away from its cathode edge.

All beam properties are lost in the glow, the motion of electrons becoming random. A small electric field extends from the anode end of the glow to the anode.

The Faraday dark space may be regarded as a modified repetition of the cathode dark space. Electrons are pulled out of the glow by the weak field and after moving a considerable distance gain sufficient random energy to excite and ionize; this point marks the head of the positive column. There is a fundamental difference between two dark spaces : in the cathode dark space there is little excitation because the electrons move fast, in the Faraday dark space they are too slow.

In the uniform positive column the axial component of the electric field is found to be constant at any point. It follows that the net space charge is zero. The weak field sustains a small rate of ionization due to the random motion of electrons. The charges flow radially by an ambipolar process to the walls where they recombine at a rate equal to their rate of production. Because of the small mobility of positive ions the electrons carry practically the whole discharge current. The attraction of electrons and the repulsion of positive ions by the anode results in a negative space charge and an enhanced field in front of the anode. This produces anode fall potential. Measurements in the anode fall and cathode fall potentials are tabulated by Brown (22). In the short region of anode fall additional

ionization occurs so that ions are fed into the positive column in numbers just sufficient to balance those that flow out of the column into the Faraday dark space.

The situation is more complicated in a striated column, although same general principles apply. There is no convincing explanation for the cause of striations.

3.2 THE POSITIVE COLUMN

3.2.1 General Features

The current in the positive column is mainly carried by electrons because of the small mobility and drift velocity of the positive ions. When the positive column is first set up, electrons will diffuse quickly to the walls, and the walls acquire a negative potential with respect to axis. The resulting space charge field, after some time will retard the electron diffusion and increase the ion diffusion so that space charge neutrality is maintained at all points in space. This is ambipolar diffusion; under this condition the electrons and ions will diffuse at the same rate as determined by the ambipolar diffusion coefficient

$$D_a = \frac{D_e\mu_+ + D_+\mu_e}{\mu_e + \mu_+} \qquad (3.2)$$

where, D_e, D_+ are electron and ion diffusion coefficients

μ_e, μ_+ are electron and ion mobilities.

Also for a Maxwellian distribution of electrons

$$\frac{D_e}{\mu_e} = \frac{kT_e}{e} , \qquad (3.2)$$

where $\mu_e = \frac{W}{E}$ (W is the drift velocity) .

This is known as Einstein's relation.

In the usual cases of interest $D_e >> D_+$ and $\mu_e >> \mu_+$ and so

$$D_a = D_+ = \frac{kT_e}{e} \mu_+ \quad (T_e >> T_+) \qquad (3.2a)$$

3.2.2 Theory

Any elementary theory of positive column gives a good quantitative description of the relations between the axial and radial electric field, the pressure, the tube radius, and the nature of the gas. Theories of the positive column apply only to certain approximate ranges of pressure, radius etc. viz., p = 0.1 to 10 torr, R = 1 to 10 cms, i = 10^{-4} to 1 amp. At lower currents the rate of ionization is too small to maintain the plasma property neutral; at higher currents gas heating becomes appreciable. Theory is based on the following premises :

(i) at every point $n_+ = n_e = n$

(ii) volume reambination is negligible

(iii) ionization is simple, not cumulative

(iv) $\lambda_e \ll R$

(v) n at walls is zero

(vi) constant electron temperature across discharge

Only that part of the theory yielding expressions for the radial distribution of charges and electron temperature, which are relevant here, is discussed. For a detailed and complete analysis one is referred to von Engel (1) and Francis (7).

(i) The radial distribution of charges

Let us consider the elementary volume shown in Fig. 3. The number of ion pairs entering the volume element dr radially per unit length of the cylinder is

$$\left(\frac{dN}{dt}\right)_r = -2\pi r l \, D_a (dn/dr)_r \qquad (3.3)$$

The number leaving dr is

$$(dN/dt)_{r+dr} = -2\pi(r+dr) l \, D_a (dn/dr)_{r+dr} \qquad (3.4)$$

where D_a is the coefficient of ambipolar diffusion and n is concentration of ions and electrons. Since for reasons of symmetry and absence of recombination in the gas $\frac{dn}{dt} = 0$ at $r = 0$, we know that its value must increase with r.

Rate of loss at the volume is given by

Rate of loss $= -2\pi r\, D_a (dn/dr)_r + 2\pi(r+dr)\, D_a (dn/dr)_{r+dr}$ (3.5)

$$= 2\pi\, D_a \left[r \frac{d^2 n}{dr^2} + \frac{dn}{dr} \right] dr \tag{3.6}$$

This number has to be balanced by ionization in the same element dr. Let each electron makes z collisions per sec.

Rate of production $= z.n.2\pi r dr$ (3.7)

Equating eqns. (3.6) and (3.7)

$$\frac{d^2 n}{dr^2} + \frac{1}{r} \frac{dn}{dr} + \frac{z}{D_a} n = 0 \tag{3.8}$$

The solution is zero order Bessel function,

$$n = n_o\, J_o\, (r \sqrt{(z/D_a)}\,) \tag{3.9}$$

when

$r\sqrt{(z/D_a)} = 2.405$, $J_o = 0$ and for larger values of $r\sqrt{(z/D_a)}$, J_o would be negative.

Since the concentration is a positive quantity, this would have no physical significance. We use the largest value of r(r = R) and impose the boundary condition

$$R\sqrt{(z/D_a)} = 2.405 \tag{3.10}$$

Substitution of this in (3.9) gives radial concentration :

$$n_r = n_o\, J_o(2.405\, \frac{r}{R}) \tag{3.11}$$

The concentration of charges in a column thus varies with r in a nearly parabolic manner. If the positive column is bounded by two parallel walls, a cosine distribution of charge is found.

(ii) The electron temperature

The energy distribution of electrons in a gas moving in an electric field and interacting strongly is approximately Maxwellian. It is thus legitimate to talk about the temperature T_e of the electron gas. Both D_a and z depend on T_e,p, and the nature of the gas. The energy distribution of electrons is

$$n(v)dv = \frac{4n_e}{\sqrt{\pi}} (v/v_m)^2 \, e^{-(v^2/v_m^2)} \, d(v/v_m), \qquad (3.12)$$

where v_m is the most probable velocity, defined by

$$\frac{1}{2} m v_m^2 = k T_e$$

or, what is identical (3.13)

$$\frac{1}{2} m \bar{v}^2 = \frac{3}{2} k T_e$$

Rate of ionization per electron is

$$z = \int_{V_i}^{\infty} F(V) \frac{dn}{n} = ap \frac{m}{e\sqrt{\pi}} a \left(\frac{2kT_e}{m}\right)^{3/2} e^{-\frac{eV_i}{KT_e}} \left[1 + \frac{1}{2} \frac{eV_i}{kT_e}\right] \qquad (3.14)$$

where F(V) is energy distribution of electrons.

After complicated steps this reduces to

$$z = 600(2/\pi)^{1/2}\ ap(e/m)^{1/2}\ V_i^{3/2}\ x^{-1/2}\ e^{-x}\ , \qquad (3.15)$$

where

$$x = eV_i/kT_e\ ;$$

a in $Volts^{-1}$, but V_i and e/m are in e.s.u.

From equation (3.10)

$$z/D_a = (2.4/R)^2 = \frac{ap^2(e/m)^{1-2}\ V_i^{1/2}}{(\mu_+\ p)}\ x^{1/2}\ e^{-x}\ , \qquad (3.16)$$

recalling the Eqns. (3.2a).

Or,

$$\frac{e^x}{x^{1/2}} = 1.2\cdot 10^7\ (cpR)^2 \qquad (3.17)$$

where

$$x = \frac{eV_i}{kT_e} \qquad (3.18)$$

and

$$c = \left(\frac{aV_i^{1/2}}{\mu_+\ p}\right) \qquad (3.19)$$

where a is the efficiency of ionization.

Expression (3.17) is the relation between T_e and (pR) for all gases. Equations (3.11) and (3.17) will be used to theoretically calculate the number density of electrons at an r and electron temperature.

3.2.3 Influence of a Magnetic Field on the Positive Column

The basic effect of a magnetic field is to cause charged particles, not already moving parallel to it, to describe helical paths. Motion of ions and electrons in a magnetic field has been treated by Allis (6) in detail. The radius of the helix decreases with increasing magnetic field. In most circumstances only the paths of electrons are altered, the ions being virtually unaffected. The electrons thus move a much longer total distance in the gas in order to move a given distance in the direction of the electric field.

A transverse magnetic field bends the positive column towards the wall of the tube. The loss of charged carriers and hence the potential required to maintain the column increases, and sufficiently large magnetic field can put out the discharge. Beckman (10) has calculated in detail the relations between the gradient, electron temperature and mean free path, and also the new electron density distribution when a cylindrical plasma is placed in a uniform transverse magnetic field. In a longitudinal magnetic field losses by radial diffusion to walls are reduced and the column can be sustained with a smaller gradient.

In conclusion of this chapter, it should be mentioned that a good account of diagnostic techniques for gaseous discharges is provided by Waters (23) and Bastien (24).

CHAPTER 4

THEORY

4.1 INTRODUCTION

In this chapter breakdown characteristics of gases in a magnetic field perpendicular to the electric field in the discharge tube, theory of equivalent-pressure-concept (EPC) and theory of simple Langmuir probe are presented. The literature on EPC is limited so the survey of it is not separately discussed but whatever important works on this field were found are quoted in appropriate places. The literature on probe theory as well as its application is so vast that many of the even most important and relevant ones cannot be quoted completely. For an interested worker, an extensive collection of literature and publications on both the above mentioned fields done by Balaraman (25) can be of help.

It is known that the breakdown of and conduction of electricity through a gas are due to charged particles (electrons, ions) in the gas. Multiplication of primary electrons leads to breakdown of the gas and after breakdown it is again charged particles that control the properties of the ionized or conducting gas. When a magnetic field is applied to an ionized gas, as in a discharge tube, the motion of charged

particles is modified in such a way that the particles, not already moving parallel to the field, will be describing cycloidal paths. The influence of longitudinal and transverse magnetic fields on a positive column was briefly discussed in the previous chapter. In a pre-breakdown situation, an applied magnetic field alters the breakdown potential. Here the discussion will be centred around only the effect of transverse magnetic field (referred to as crossed-fields) on pre-discharge and post-discharge conditions. For breakdown of a gas, a transverse magnetic field affects the process in such a way that the pressure of the gas is apparently increased. In other words, in the absence of the field, the same discharge characteristics as in the field can be observed if only the pressure of the gas is increased by the apparent increase of pressure due to the applied field. This is known as equivalent-pressure-concept. That is, application of a transverse magnetic field to a discharge tube before breakdown is equivalent to increasing the gas pressure in the tube.

The simplest Langmuir probe or electrostatic probe is an auxiliary electrode inserted into the plasma and having dimensions much smaller than those of the main electrodes or radius of the tube. The theory of an electrostatic probe was first developed by Langmuir and Mott-Smith (18). Various potentials are applied to the probe and corresponding collection currents

are measured to determine free charge concentrations and electron temperature. The conditions under which a Langmuir probe is applicable and modified expression in a short-mean-free-path conditions will also be discussed.

4.2 GASEOUS BREAKDOWN IN CROSSED MAGNETIC FIELD AND EQUIVALENT PRESSURE CONCEPT

The theory of electron drift in a gas under the combined action of electric and magnetic fields was first developed by Tonks and Allis (8), an improved theory of earlier inexact theories. Transport of charged particles and drift of electrons were experimentally investigated by many workers like Bernstein (26) and Fletcher and Haydon (27). Later with the use of the theory developed by Allis, Heylen and Dargan (28) calculated electron drift velocities in hydrogen, nitrogen, oxygen, and air. Measurements of Townsend's first ionization coefficient for various gases, in crossed-fields were carried out by Blevin and Haydon (13), Bernstein (26), Gurumurthy and Raju (29), and many others. It was Blevin and Haydon (13) who first introduced the equivalent-pressure-concept and also gave the treatment of the transport and ionization coefficients. EPC was later substantiated by the experiments carried out by Haydon and Robertson (30), Dargan and Heylen (14), Bhiday et al (31), Sengupta et al (17), and many others. Though, as pointed out by Haydon (15), the theory is not exact, it applies to certain ranges of E/p and H/p effectively.

4.2.1 The Influence of a Transverse Magnetic Field on the Electron Avalanche

Earlier workers (12,32) examined the problem through the study of individual electron trajectories in the gas. While qualitative agreement with experiment was reasonably good, quantitative agreement was far from satisfactory. A new approach was made by Blevin and Haydon (13) and consideration was given to the 'bulk' properties of the electron avalanches, such as electron mean energy, drift velocity and the distribution function for the electron energies.

In the absence of magnetic field, the bulk approach leads to the following expression for the first Townsend coefficient,

$$\frac{\alpha}{p} = KW^{-1} \int_0^\infty P(v)\, v^{1/2}\, f(v)\, dv \qquad (4.1)$$

where $K = (e/150m)^{1/2}$ and is a constant

W is the electron drift velocity

$P(v)$ is the ionization efficiency of electrons with energy v, at 1 torr pressure, and

$f(v)$ is the energy distribution function of the electron

In order to extend this approach to the case when a transverse magnetic field is present, it is necessary to determine the influence of the magnetic field on the quantities occurring on RHS of Eqn. (4.1). One may then obtain a new expression for α/p as a function of H/p and E/p.

To study this problem, it is necessary to know the variation of the mean free path l with electron velocity v. The assumption usually made is that l is independent of v, and for some gases (notably air) this is approximately valid. However, for many gases l is proportional to v. Another assumption is that l/v ($= \tau$, the mean free time) is constant for a given pressure. When only electric field is present, any quantity Q under discussion will be denoted by Q_{O}, E/p; when both H and E are present, the quantity will be denoted by $Q_{H/p,E/p}$.

When τ is constant, the drift velocity is given by

$$W_{O,E/p} = \frac{Ee\tau}{m} \qquad (4.2)$$

An expression for $W_{H/p,E/p}$ in the presence of magnetic field has been obtain by Blevin and Haydon (13). Assuming that $l = f(v)$ and, for particular case when $l/v = \tau$:

$$W_{H/p,E/p} = \frac{E}{H} \cdot \frac{\tau\omega}{1+\omega^2\tau^2} \qquad (4.3)$$

where

$$\omega = \frac{e}{m} H$$

From (4.2) and (4.3)

$$W_{O,E/p} = W_{H/p,E/p}(1+ \omega^2 \tau^2)$$

$$W_{O,E/p}/W_{H/p,E/p} = 1+ \omega^2 \tau^2 \qquad (4.4)$$

Also $\tau = Hel/mpv$, so that for a given gas

$$\omega^2 \tau^2 = C(H/p)^2, \qquad (4.5)$$

where C is a constant,

$$C = (el/mv)^2 \qquad (4.6)$$

Substituting for $\omega^2 \tau^2$ in (4.4),

$$W_{O,E/p}/W_{H/p,E/p} = 1+C(H/p)^2 \qquad (4.7)$$

The precise form of velocity distribution of electrons in crossed electric and magnetic fields is not known, except for the particular case when the collisions between electrons and gas molecules are elastic. For an equilibrium condition one can derive the expression

$$p'/p = W_{O,E/p'}/W_{H/p,E/p} \qquad (4.8)$$

$$p'/p = W_{O,E/p'}/W_{H/p,E/p} \qquad (4.9)$$

$$= \left(\frac{W_{O,E/p'}}{W_{O,E/p}}\right)\left(\frac{W_{O,E/p}}{W_{H/p,E/p}}\right)$$

Now from Eqn. (4.2)

$$\frac{W_{O,E/p'}}{W_{O,E/p}} = \frac{p}{p'} \text{ , so that}$$

$$\frac{p'}{p} = \sqrt{\left(\frac{W_{O,E/p}}{W_{H/p,E/p}}\right)} \tag{4.10}$$

Using (4.7)

$$p' = p[1+C(H/p)^2]^{1/2} \tag{4.11}$$

From the definition of p' it follows that in crossed electric and magnetic fields the electrons behave energetically as they would if only electric field were present, and the pressure were increased from p to p'.

Now for first Townsend ionization coefficient it can be easily shown that

$$(\alpha/p)_{H/p,E/p} = \frac{p'}{p} \left(\frac{\alpha}{p}\right)_{O,E/p} \tag{4.12}$$

This is on the assumption that the magnetic field does not alter the form of the distribution function.

For a given cathode surface, γ will depend only upon the energy of positive ions reaching the cathode. However, magnetic field has little effect on the motion of positive ions owing to

their much greater mass. The 'equivalent pressure' for the ions is very little different from the actual pressure, except for large values of H/p.

With this restriction,

$$\gamma_{H/p,E/p} = \gamma_{O,E/p} \tag{4.13}$$

The effective electron molecule collision frequency is given as

$$\nu = \frac{vp}{l} \tag{4.14}$$

where l is mean free path at 1 torr.

From Eqn. (4.11) it readily follows that

$$p' = p[1 + \frac{\omega^2}{\nu^2}]^{1/2} \tag{4.15}$$

where ω is the cyclotron frequency given as

$$\omega = \frac{e}{m} H .$$

4.2.2 Sparking in Crossed Magnetic Field

When a magnetic field is applied to a gap, the electron swarm is deflected through an angle θ, so that the electric field along which the electrons travel is reduced to E cos θ. At the same time, the path length is increased, so that the number of ionizations in the electric field direction is

increased by $(\cos\theta)^{-1}$. Taking these two factors into consideration Eqn. (2.7) becomes

$$\left(\frac{\alpha}{p}\right)_{H/p} = \frac{A}{\cos\theta} \exp\left(-\frac{Bp}{E\cos\theta}\right) \tag{4.16}$$

so that the sparking voltage is given by

$$(V_s)_{H/p} = \frac{Bpd\sec\theta}{\ln(pd\sec\theta) + \ln\left[\frac{A}{\ln(1+\frac{1}{\gamma})}\right]} = V_{so}\sec\theta \tag{4.17}$$

Assuming that the electron-energy distribution remains Maxwellian and that the collision frequency ν is independent of electron energy, Heylen (11) and Allis (6) have shown that the perpendicular (to both electric and magnetic fields) electron velocity v_p and transverse (along electric field direction) velocity v_T are given by

$$v_p = \frac{e}{m} E \frac{\omega}{\nu^2 + \omega^2} \tag{4.18}$$

$$v_T = \frac{e}{m} E \frac{\nu}{\nu^2 + \omega^2} \tag{4.19}$$

The angle of deflection is given as

$$\tan\theta = \frac{v_P}{v_T} = \frac{\omega}{\nu} \tag{4.20}$$

and thus

$$\sec\theta = [1+(\frac{\omega}{\nu})^2] = [1+(\frac{e}{m}\frac{H}{\nu_o p})^2]^{1/2} \qquad (4.20)$$

Combining Eqns. (4.17) and (4.21) one finds that the sparking voltage is solely a function of pd and of H/p.

It is clear that a crossed magnetic field increases effectively the gas pressure from p to psecθ. Thus the sparking characteristics have the following form. When pd is smaller than $(pd)_{min}$, application of moderate magnetic field increases pd, and hence the sparking voltages will decrease until it approaches a minimum value and it also intersects the H = O field line; with further increase in magnetic field V_s will begin to rise again. For high magnetic fields, the Paschen curves do not intersect the H = O curve. Beyond the minimum value of V_s, which corresponds to the right-side of Paschen curve, the application of medium or strong magnetic field will effectively increase pd, hence will always result in an increase in the sparking voltage. Making use of the EPC and of the fact that the effective field $E_{H/p}$ is E cosθ,

$$E_{H/p} = E[1+(\frac{\omega}{\nu})^2]^{1/2} \qquad (4.22)$$

It is to be borne in mind that the underlying assumptions in the above treatment are : (i) magnetic field does not

alter the electron energy distribution; (ii) the electric field is uniform; (iii) there is no influence on secondary ionization coefficient. These are valid only when H/p is small. The deviation at strong magnetic fields has been discussed by Haydon (15). The condition for low and high magnetic field is determined by

$$\nu_o^2 \quad \begin{matrix} >> \\ << \end{matrix} \quad \left(\frac{e}{m}\frac{H}{p}\right)^2 \tag{4.23}$$

ν_o - collision frequency at unit pressure.

4.2.3 Electron Molecule Collision Frequency

In order to determine the influence of a crossed magnetic field on the sparking voltage, it is necessary, through Eqns. (4.17) and (4.21), to know the collision frequency ν of the electrons in the particular gas. This quantity can also be measured from pre-breakdown ionization currents (30). Dargan and Heylen (14) introduced the method of determining ν from sparking-voltage data.

Returning to Eqn. (4.17), if, with an increase in magnetic field, the sparking voltage can be maintained constant, then the product $pd\sec\theta$ remains constant and is equal to $(pd)_o$ in the absence of a magnetic field. Thus making use of Eqn. (4.21),

$$(pd)^2 + (pd)^2 \left(\frac{e}{m}\frac{H}{\nu}\right)^2 = (pd)_o^2 \tag{4.24}$$

For this equality to hold, either the d or p must be decreased with an increase in H. When p is kept constant and d is varied (4.30) becomes

$$d^2 = -\left(\frac{e}{m\nu}\right)^2 (Hd)^2 + d_o^2 \qquad (4.25)$$

If d is kept constant and p is varied

$$p^2 = -\left(\frac{e}{m\nu_o}\right)^2 H^2 + p_o^2 \qquad (4.26)$$

Eqns. (4.25) and (4.26) are straight lines, the slopes of which would determine the collision frequency. The influence of the magnetic field is more marked at low pressures because the collision frequency increases with pressure and E/p is also very large. For pd greater than the critical value, the sparking voltage is increased in accordance with the EPC, except at large H/p, where the discharge moves into non-uniform electric field.

4.3 THE INFLUENCE OF A TRANSVERSE MAGNETIC FIELD ON A DISCHARGE PLASMA

When a magnetic field acts upon a glow discharge, various changes such as increase of equivalent pressure, decrease in the length of the cathode dark space, a change in radial charge density in the positive column and marked changes in the V-I characteristics of the discharge take place. Magnetic field

also causes an increase in electron temperature and the axial field strength. Formulae relating the axial electric field, the magnetic field and the electron temperature have been derived by Beckman (10). Most of the experiments has been done in a longitudinal magnetic field.

It is possible to deduce from the treatment of Beckman (10) the variation of a discharge current in a magnetic field. The experimental study of this variation has been done by Sen and Gupta (33). They observed that the gases showed a gradual rise of the discharge current with the magnetic field, attaining a maximum value (I_{max}) at a particular value of H and decreasing gradually. They also made the following observations :

(i) irrespective of the nature of the gas, the magnetic field at which the discharge current becomes maximum (H_{max}) is the same for all the gases provided that the initial discharge current (I_o) is the same, and it is independent of pressure;

(ii) $(H_{max})^2$ is proportional to I_o;

(iii) for same I_o, $I_{max}p$ is constant.

By the use of Beckman's treatment, they derived an expression for H_{max} as

$$H_{max} = 12.41 \times 10^{-2} \left(\frac{T_e}{K}\right)^{1/2}, \qquad (4.27)$$

where K is the fraction of energy lost by collision, and

T_e is the electron temperature.

4.4 LANGMUIR PROBE

Since the original work of Langmuir and Mott-Smith (18), probes have been extensively used for the study of plasma properties in low pressure gas discharges (34,35,36,37). An electrostatic or Langmuir probe is a small auxiliary electrode of dimension much smaller than the dimensions of electrodes in a discharge tube. The electron and positive ion densities, the electron temperature, and the plasma potential are determined from the volt-ampere characteristics of the probe called the 'probe characteristic'. There are three types of Langmuir probe, based on their shape namely plane, cylindrical, and spherical. In this section general features of a current collector (such as probe), its theory (centered around cylindrical probe), and the limitations of application will be discussed.

4.4.1 General Features

A probe is immersed in a plasma and its potential varied with respect to the surrounding plasma potential. In the discussion we analyse the problem from negative bias and moving to positive bias. When the collector is negatively biased, it repels electrons from its neighbourhood but gathers positive ions. It thus becomes surrounded by a positive ion sheath or region which contains a positive ion space charge, but no free electrons. The whole drop in potential between the ionized gas and the collector becomes concentrated within this sheath, the

positive space charge on the ions in the sheath being able to neutralize the effect of the negative charge on the electrode so that the field of the collector does not extend beyond the outer edge of the sheath. The number of ions taken up by the collector is thus limited by the number that reaches the outer edge of the sheath. The thickness and thus the area of the outside the sheath can be calculated from space charge equations. The current density over this area measures the positive ion current density in the ionized gas.

In a similar manner a positively biased electrode of small size becomes surrounded by an electron sheath, and the current under these conditions is limited by the rate at which the electrons reach the edge of the sheath. Because of the small mass and consequent high mobility of electrons, the electron current densities in uniformly ionized gases are hundreds of times greater than the positive ion current densities. If the collector is at a potential slightly negative with respect to the space, electrons may still reach the electrode if they have sufficient velocities to carry them against the retarding field. As the collector is made more negative, the lower speed electrons fail to reach the collector, although those with high speed may still reach it. The volt-ampere characteristics of a collector therefore gives indications as to the distribution of velocities among the electrons in the ionized gas.

A very common type of velocity distribution is random type usually known as the Maxwellian distribution. When the electron velocities have this distribution the electron current flowing to any collector at a potential V, which is negative with respect to the surrounding space, is given by the equation

$$i = IA \exp(eV/kT_e) \qquad (4.28)$$

where I is the electron current density

A is the area of the collector

T_e is the absolute temperature of electrons.

4.4.2 Collector with Retarding Field

Equation (4.28) is derived from Boltzmann equation describing the electron density as,

$$n'/n = \exp(-E/kT) \qquad (4.29)$$

In a state of equilibrium and among particles which have a Maxwellian distribution of velocities, the ratio of the concentrations of the particles in two regions where the potential energies of the particles are different is given by Boltzmann equation. n' and n are the number of particles per unit volume in the two regions and E is the work which must be expended in bringing a single particle from the second region (corresponding to n) to the first region. If we consider the

particles as electrons, the Boltzmann equation becomes

$$n'/n = \exp(Ve/kT_e) \qquad (4.30)$$

Let us now consider a negatively charged collector surrounded by ionized gas containing n electrons per unit volume moving with Maxwellian velocities corresponding to a temperature T_e. Let us also assume provisionally that the surface of the collector is a perfect reflector in regard to electron impacts, so that all electrons which strike it rebound elastically, and the current to the collector is zero. Then it is clear that the presence of the collector will not disturb the condition of equilibrium corresponding to the Maxwellian distribution, and the Boltzmann equation can be used to calculate the electron densities within the positive ion sheath enveloping the collector. If V is the potential of the collector with respect to the surrounding ionized gas, then n', the number of electrons per unit volume in an element of space right at the surface of the collector, is given by Eqn. (4.30). Considering an imaginary plane in the body of the ionized gas, the current density of electrons passing per sec per unit area through this plane is given by

$$i = 1/4\ nve \qquad (4.31)$$

where v is the average velocity of electrons.

Equation (4.28) thus gives the current of electrons which strike the surface of the collector under the conditions assumed: Maxwellian distribution and perfectly reflecting collector. Taking the natural logarithm of Eqn. (4.28) we get

$$\ln i = \text{const} + \frac{Ve}{kT_e} \qquad (4.32)$$

Thus if we plot the logarithm of the electron current i as a function of the potential V of the collector, we should obtain a straight line of slope e/kT_e.

4.4.3 Collector with Accelerating Field

Equation (4.28) does not apply when the potential of the collector is such as to exert an attractive force on the particles being collected. The Boltzmann equation should apply for equilibrium conditions regardless of the polarity of the electrode, so that for a perfectly reflecting collector (4.28) would give the current of electrons striking the surface even with an accelerating field. But increase in current density near the electrode, as compared with that further from it, is then due to the large number of low velocity electrons, resulting from collisions, which are trapped within the region around the collector by the accelerating field which prevents their escape. Also the accelerating field causes the paths of the electrons to curve inwards as they approach the collector so that the current collected is greater than A . When the sheath

radius (a) is large compared to that of the collector and especially when the initial velocities of the electrons or ions are high the orbital motion of the particles must be considered. There are cases where the potential distribution around the collector can affect the current that flows. For example, with a field of force limited to a sheath of radius a, the current collected by a cylinder of length l certainly cannot exceed $2\pi al$. So we have conditions of currents : (i) currents limited by the sheath area or (ii) currents limited by orbital motion. The factor a/r_p (r_p is probe radius in a cylindrical case) decides which condition prevails. With this background we will discuss ion and electron densities in the next section.

4.4.4 Deduction of Plasma Parameters from Probe Characteristic

A typical probe characteristic is shown in Fig. 4. It is customary to divide the probe curve into three parts: the positive ion saturation, the region of partial collection of electrons, and the electron saturation.

When the probe potential is sufficiently negative with respect to the plasma in which the probe is inserted, the probe will attract positive ions and repel all electrons and thus the probe current consists only of positive ions. This is called positive ion saturation. In the vicinity of the probe, only positive ions contribute to the space charge and the

potential is a steep function of position. At larger distances from the probe both electrons and positive ions contribute to the space charge and the electric fields are small. Region A in Fig. 4 can be referred to.

As the magnitude of the voltage on the probe with respect to plasma potential is decreased, the probe starts collecting electrons. When the probe attains the floating potential V_f, equal numbers of electrons and ions flow. As V increases further, the probe collects more and more electrons. The straightness of the region OB (when ln i is plotted against V) shows the electron velocity distribution is Maxwellian. At still higher potential the electron current saturates. This is called plasma potential. At plasma potential, all the electrons hitting the probe are collected. At plasma potential, the probe is not covered by a sheath of electrons and ions reach the probe by diffusion.

a) Ion current :

In the last section it was assumed that no electric field penetrates from the probe beyond the sheath edge and both electrons and ions have a Maxwellian velocity distribution at the sheath edge. Under these assumptions the random ion current density, J_r, reaches the sheath edge. It is given by

$$J_r = en_+ (kT_+/2\pi M)^{1/2} \qquad (4.33)$$

where T_+ is positive ion temperature

M mass of the ion and

n_+ ion density.

The assumption of a Maxwellian velocity distribution for positive ions at the sheath edge is unsatisfactory because equilibrium is disturbed near the sheath by the drain of ions to the probe. Small electric fields and density gradients may penetrate beyond the sheath and cause a drift current of positive ions at the sheath edge. It is necessary to take this into account.

The current density of positive ions at any point in the sheath, including the drift current at the sheath edge is given as

$$J_d = en[(\frac{2e}{M})\ (V+\omega)]^{1/2}\ , \qquad (4.34)$$

where V is the potential at any point in the sheath

ω the directed energy of ions reaching the sheath edge

n ion density at any point.

When a Boltzmann distribution for electrons is justified, J_d can be deduced as

$$J_d = en_s(\frac{kT_e}{M})^{1/2}\ , \qquad (4.35)$$

and is thus proportional to the electron temperature.

Thus the penetrating electric field imparts to the ions a drift velocity $(kT_e/M)^{1/2}$. This has assumed that there are no collisions in the sheath. When there are collisions the expressions for current densities would differ. Collisions in the vicinity of the probe occurs when the mean free path of electrons is short compared to the probe radius. A continuum theory has been derived for a cylindrical probe by Zakharova et al (37). They have given an expression for ion current density at the probe surface as

$$(J_+)_p = 3.2\left(\frac{\lambda_+}{r_p}\right) [J_+/\ln (L/r_p\, x_o)] \qquad (4.36)$$

where λ_+ is ion mean free path

J_+ is random ion current flux in the body of the plasma

L is length of the probe

x_o is normalized sheath size.

J_+ is given by the Eqn. (4.33).

Because the ions are accelerated in the region of field penetration, ion temperature cannot be determined. Ion density can be determined by the use of the expression (4.36).

b) Electron current :

Because the plasma electron-energy distribution is generally Maxwellian in the region OB of the characteristic, the electron concentration n_{ep} at the probe surface relative to that in the plasma can be written as

$$n_{ep} = n_{eo} \exp(-\frac{eV_p}{kT_e}) \qquad (4.37)$$

where

V_p is the probe potential

n_{eo} is electron concentration in the plasma

Thus the electron current density to the probe is given by

$$J_{ep} = J_e \exp(-\frac{eV_p}{kT_e}) \qquad (4.38)$$

The plasma electron current density J_e is given as

$$J_e = \frac{1}{4} en_{eo} \bar{v} \qquad (4.39)$$

where $\bar{v}$ is the mean electron velocity.

At plasma potential Eqn. (4.47) can be written as

$$J_{ep} = J_e = \frac{1}{4} en_e (\frac{8kT_e}{\pi m})^{1/2} \qquad (4.40)$$

where

$n_e = n_{eo}$ (for convenience)

m is the electronic mass

T_e is the electron temperature

k is Boltzmann constant

e is the electronic charge .

Eqn. (4.48) is used to determine the electron density by knowing the current density to a probe. When the plasma is

collision dominated plasma (a true situation) and when the mean free path of electrons is comparable or less than the probe radius the electron current density at the probe is modified as

$$(J_e)_p = \frac{J_e}{1+\frac{3}{4}\left(\frac{r_p}{\lambda_e}\right)\ln\frac{L}{r_p}} \quad \text{(at plasma potential)} \qquad (4.41)$$

where

$(J_e)_p$ is the current density at the probe (V_p = plasma potential)

J_e is the random current density in the plasma

L is the length of the cylindrical probe

r_p is the radius of the probe

λ_e is the electron mean free path.

Expression (4.50) is used to calculate the electron density Eqn. (4.40) is used to measure the electron temperature, that is,

$$\frac{d(\ln J_e)}{dV} = \frac{e}{kT_e} \qquad (4.42)$$

when the slope is in volt^{-1}, T_e is obtained in absolute temperature.

In the derivation of simple Langmuir probe, many assumptions were considered : the energy distribution is Maxwellian ; there are no collisions in the sheath; plasma

is not disturbed by the presence of probe; probe is perfect reflector of plasma, There are experimental situations where the energy distribution is non-Maxwellian. There are collisions at higher pressures. When collisions are considered, the expressions for plasma parameters are modified. However, a new method of Langmuir probe analysis has been proposed by Cellarius et al (38). Also, when using Langmuir probes in a non-Maxwellian plasma, numerical or electronic double differentiation is used to obtain the distribution function by Druyvesteyn method, which consists of a determination of the second derivative of the probe current with respect to voltage, relative to plasma potential. Maxwellian distribution is certainly probable in a discharge tube when (i) E/p is low, in which case the electron mean free path and collisional energy loss are independent of energy, and (ii) electron density is high (10^{12} cm^{-3}), where short range electron-electron interaction is then possible. Many probe investigators suggest that the Maxwellian distribution is valid for electron densities in the range of 10^{9} to 10^{12} cm^{-3}.

Before ending this chapter it is to be mentioned that the double probe technique developed by Johnson and Malter (39) in many situations where Langmuir probe fails, particularly when a large reference electrode is absent or when the space potential is not well defined. Though there are many assumptions underlying in the Probe theory, Langmuir probe has been found giving accurate results in a plasma laboratories.

CHAPTER 5

EXPERIMENTAL SETUPS

Main objectives of this work are : (1) to study the effect of transverse magnetic field on breakdown potential through Paschen curves, and to determine electron-molecule collision frequency from breakdown data; (2) to study the variation of discharge current in a transverse magnetic field; and (3) to determine the electron temperature and density in the positive column of glow discharge.

5.1 TO STUDY BREAKDOWN IN TRANSVERSE MAGNETIC FIELD

5.1.1 Apparatus

The experimental arrangement is schematically shown in Fig. 5. Four discharge tubes with four different electrode materials - SS, copper, brass, aluminium - are made, which are 4 cm in diameter. All the electrodes are plane and circular and of the same dimension of 2.5 cm dia. The anode of the tubes is sealed to glass with torseal, whereas the cathode is movable and provided with a long stem, which passes through an SS bellow to the farther end. Compressing of the bellow, done by a screw, causes the electrode (cathode) to move. The bellow is supported horizontally on a trolly. To one end of the bellow the discharge tube is set with flange and O-ring arrangement as shown in the figure. When the experimentation

is finished with one tube, it is removed and another tube of different electrode can be set for doing the experiment. Anodes and cathodes are washed with n-hexane to remove any grease on them. The gap distance can be varied from 0.5 cm to 4 cm, and it is measured with a traveling microscope.

The base vacuum in the set up can reach is 0.04 torr. The pressures below 0.5 torr are measured with a Pirani gauge, and 1 torr and above are measured with a calibrated, closed U-manometer. The leakage rate of the arrangement is 0.05 torr/5 min at 0,05 torr, 0.1 torr/15 min at 0.2 torr, and 1 torr/10 hr at 1 torr. Manometer level is measured with a traveling microscope. An electromagnet with plane pole pieces provides magnetic field. With poles at a gap of 6 cm, this produces a field of 4000 Gs (0.4 Tesla) when a current of 4A flows to the coils.

5.1.2 Procedure

The electrical circuit to measure the breakdown potential is shown in the inset of Fig. 5. Motwane multimeters are used to measure the potential and current. The Fluke DC power supply can provide the potentials from $\pm$ 0 to $\pm$ 2500 V. Breakdown potential is measured as the potential across the electrodes when a constant current of 5×10^{-7} A flows through the tube. When discharge takes place, spikes are also seen in the oscilloscope.

5.3 TO CONSTRUCT A LANGMUIR PROBE AND USE IT TO DETERMINE PLASMA PARAMETERS

5.3.1 Probe Construction

The construction of Langmuir probe is schematically shown in Fig. 6. A tungsten wire 20 mil thick and 5 cm long - is spot-welded to a long copper wire. The tungsten wire is fused to a narrow glass tube - the wire is 4 cm long from the fuse. The glass tube is encapsulated by a steel tube of 9 mm dia, and the glass tube is sealed to the steel tube at both ends with torseal. A teflon rod with double O-ring is fabricated for translatory motion of the probe. The steel tube passes through the O-rings and is fixed to the rotor. Leaving a small length at the tip, the remaining length of the tungsten wire is coated with silica. The total diameter of the coated portion is around 2.5 mm. Effective probe length is measured as 2.43 mm.

5.3.2 Procedure

The discharge tube for the use of Langmuir probe is different from that for magnetic field study, and is of silica glass of 5.1 cm inner dia with nickel electrodes of 4 cm dia separated by 25 cm. The probe, along with the teflon translator, is fixed with torseal at the centre of the discharge tube. This is schematically shown in Fig. 7. The probe circuit is shown in the inset. Prior to use, the probes are cleaned by

yh
the application of -200 to -300 V (with respect to floating potential). The surface is cleaned by ion sputtering. Similarly it is cleaned by electron-bombardment by applying large positive potentials.

The desired pressure of any gas is maintained with the help of needle valve . To start with, probe is always given +200 V from the Fluke DC power supply (different from tube power supply). A discharge current of desired value is adjusted. The potential is slowly increased from + 200 V and bias voltages required for various ion currents from 4 μA to zero total current are measured. As bias is increased, the current reaches a zero value and further increases - but in the opposite direction. The polarities of the ammeter are to be changed now. Bias potentials for different probe currents are noted down until a bright glow appears around the tip.

The procedure is followed for discharge currents of 4,7,10,15,20 mA. For every current the probe is used at the axis of the discharge tube and radially 10 mm from the axis. Eight turns of the rotor of the translator gives a 10 mm - movement. The procedure is followed at various pressures : 0.2, 0.5, 1, 1.5 and 2 torr in air, argon, N_2, O_2, and CO_2 - of course not all the pressures are done with all the gases.

The results of these experiments are given in the next chapter.

CHAPTER 6

RESULTS

6.1 ELECTRON-MOLECULE COLLISION FREQUENCY

For fixed values of gap distances the Paschen curves are drawn. The Paschen curves for air are shown in Figs. 8-11, for argon , Figs. 12-15, for CO_2, Figs. 16 and 17, for H_2 in Figs. 18 and 19, for N_2 in Fig. 20, and for O_2 in Fig. 21.

The general observation is that for all gases, larger the magnetic field higher is the breakdown potential. As discussed in Chapter 4, below Paschen minimum, the moderate magnetic field of 500 Gs decreases the breakdown potential.

For the calculation of molecular frequency the governing equation used is (4.26). For constant breakdown potential, the pressures corresponding to the magnetic field settings are noted. Now for every breakdown potential p^2 is plotted against H^2. Typical plots are shown in Figs. 22 and 23. The slope gives the value of $(e/m\nu_o)^2$, from which ν_o is calculated. As seen from p^2 vs H^2 plots, for all gases, at low magnetic fields, the slope differs from that at high magnetic fields, so from every plot two collision frequencies are calculated. These are referred to as low and high corresponding to low magnetic fields and high magnetic fields. The results are tabulated in Tables 1-6.

Table 1

Electron-molecule collision frequency in air for varying magnetic fields and electrode materials

H	V_s V	E/p $Vcm^{-1}torr^{-1}$	H/p $Gs\ torr^{-1}$	$\nu_o x10^{-9}$ $s^{-1}\ torr^{-1}$	Electrode and d
1	2	3	4	5	6
	700	152	54	2.78	Brass
Low	800	137	43	2.54	d=0.5 cm
	1000	110	27	1.36	(Fig. 8)
	1200	95	20	1.05	
	700	169	241	7.87	
	800	148	185	7.87	
High	1000	118	118	7.19	(Fig. 8)
	1200	100	83	7.87	
	1200	120	50	3.11	SS
Low	1400	102	36	3.21	d=1.0 cm
	1600	93	29	2.27	(Fig. 9)
	1800	86	24	1.31	
	1200	143	238	6.65	
High	1400	117	167	5.87	
	1600	100	125	5.31	(Fig. 9)
	1800	90	200	5.31	

contd ...

contd ... (Table 1)

1	2	3	4	5	6
	1050	107	51	3.11	Brass
Low	1100	102	46	3.33	d=1.0 cm
	1200	98	41	2.07	(Fig.10)
	1400	85	30	3.32	
	1600	80	25	2.27	
	1050	131	250	6.57	
	1100	122	222	6.96	
High	1200	111	185	7.31	(Fig. 10)
	1400	95	135	6.96	
	1600	86	107	6.22	
	1500	108	55	3.11	SS
	1700	100	44	2.65	d=1.5 cm
Low	1900	92	36	2.27	(Fig. 11)
	2100	85	30	1.21	
	1500	145	290	6.38	
High	1700	126	222	5.08	
	1900	112	177	6.07	(Fig. 11)
	2100	102	146	6.22	

contd ...

contd .. (Table 1)

1	2	3	4	5	6
Low	1500	111	111	4.40	Copper
	2050	83	61	2.35	d=3.0 cm
	2150	79	54	2.44	
High	1500	167	333	4.40	Coppe5
	2050	98	143	5.31	d=3.0 cm
	2100	90	125	5.15	
	2200	89	122	5.47	

Table 2

Electron-molecule collision frequency in argon for varying magnetic fields and electrode materials

I	V_s V	E/p $Vcm^{-1}torr^{-1}$	H/p Gs $torr^{-1}$	$\nu_o x10^{-9}$ $s^{-1}torr^{-1}$	Electrode and d
	2	3	4	5	6
	450	98	54	0.89	SS
ow	500	82	41	0.67	d=0.5 cm
	600	60	25	0.48	(Fig. 12)
	650	55	21	0.36	
	450	118	263	6.65	
	500	88	175	8.21	
igh	600	62	104	5.87	(Fig. 12)
	650	56	86	5.08	
	550	65	60	1.18	SS
	650	42	38	0.98	d=1.0 cm
ow	750	41	27	0.67	(Fig. 13)
	900	33	19	0.46	
	550	86	313	6.96	
	650	51	187	7.19	
igh	750	46	123	5.08	(Fig. 13)
	900	35	78	3.94	

contd ...

contd .. 2 (Table 2)

1	2	3	4	5	6
	750	44	44	1.24	SS
	850	39	34	1.00	d=1.5 cm
Low	950	36	28	0.82	(Fig. 14)
	1300	26	15	0.67	
	750	77	308	3.78	
High	850	52	182	4.32	(Fig. 14)
	950	45	141	5.31	
	1300	33	75	2.54	
	1400	44	63	0.86	SS
Low	1500	41	555	0.77	d=4.0 cm
	1600	38	48	0.71	(Fig. 15)
	1700	37	43	0.64	
	1400	146	833	4.19	
	1500	94	500	4.11	(Fig. 15)
High	1600	69	345	4.00	
	1700	54	256	4.19	

Table 3

Electron-molecule collision frequency in CO_2 for varying magnetic fields and electrode materials

H	V_s	E/p $Vcm^{-1}torr^{-1}$	H/p $Gs\ torr^{-1}$	$\nu_o x10^{-9}$ $s^{-1}torr^{-1}$	Electrode and α
1	2	3	4	5	6
	800	314	98	6.22	SS
	900	247	68	12.44	d=0.5 cm
Low	1100	167	38	12.45	
	1500	110	19	1.19	
	800	348	435	27.85	SS
	900	257	285	22.70	d=0.5 cm
High	1100	167	152	12.45	
	1500	113	75	12.45	
	1200	154	64	1.58	Aluminium
	1400	124	44	1.37	d=1.0 cm
Low	1600	105	33	1.14	(Fig. 16)
	1800	90	25	0.95	
	1200	222	370	9.03	
	1400	157	225	8.45	Fig. 16)
High	1600	131	164	5.08	
	1800	106	118	4.27	

contd ...

contd ... (Table 3)

1	2	3	4	5	6
	1200	167	139	2.27	SS
Low	1300	148	114	2.27	d=2.0 cm
	1500	121	81	1.83	(Fig. 17)
	1700	106	63	1.92	
	1200	674	2247	11.52	
High	1300	500	1538	9.64	(Fig. 17)
	1500	268	714	22.71	
	1700	167	392	19.88	

Table 4

Electron-molecule collision frequency in hydrogen for varying magnetic fields and electrode materials

H	V_s V	E/p $Vcm^{-1}torr^{-1}$	H/p $Gs\ torr^{-1}$	$\nu_o \times 10^{-9}$ $s^{-1}torr^{-1}$	Electrode and d
	650	66	25	1.76	Aluminium
	700	60	22	1.49	d=0.5 cm
Low	750	56	19	1.19	(Fig. 18)
	800	52	16	1.61	
	650	84	129	3.11	
	700	68	98	3.27	
High	750	61	82	4.15	(Fig. 18)
	800	57	71	4.27	
	1650	40	36	2.13	Aluminium
	1800	38	31	1.97	d=3.0 cm
Low	1900	36	29	1.76	(Fig. 19)
	2000	35	26	1.61	
	1650	89	323	4.27	
	1800	60	200	3.75	
High	1900	53	267	3.33	(Fig. 19)
	2000	48	143	3.18	

Table 5

Electron-molecule collision frequency in nitrogen for varying magnetic fields

H	V_s V	E/p $Vcm^{-1}torr^{-1}$	H/p $Vcm^{-1}torr^{-1}$	$\nu_o \times 10^{-9}$ $s^{-1}torr^{-1}$	Electrode and d
Low	1050	125	60	2.78	SS
	1150	120	52	1.88	d=1.0 cm
	1300	111	43	1.88	(Fig. 20)
	1500	98	33	2.26	
High	1050	162	308	7.87	
	1150	144	250	6.65	
	1300	130	200	6.56	(Fig. 20)
	1500	113	150	5.31	

Table 6

Electron-molecule collision frequency in oxygen for varying magnetic fields

H	V_s V	E/p $Vcm^{-1}torr^{-1}$	H/p $Gs\ torr^{-1}$	$\nu_o \times 10^{-9}$	Electrode and d
Low	650	197	76	3.94	Aluminium d=0.5 cm (Fig. 21)
	750	160	53	2.54	
	900	111	37	2.27	
	1200	64	22	1.61	
High	650	236	364	9.54	(Fig. 21)
	750	183	244	9.28	
	800	115	154	7.19	
	1200	66	87	7.87	

6.2 VARIATION OF DISCHARGE CURRENT IN A MAGNETIC FIELD

The variation of discharge current when a transverse magnetic field is applied is shown in Figs. 24 and 25. As the field is increased, the current reaches a maximum and gradually decreases. The results are tabulated in Tables 7 and 8. H^2_{max}/I_o and $I_{max}p$ are calculated.

Table 7

Variation of discharge current with magnetic field in CO_2 gas for a gap distance d = 0.5 cm

Initial current I_o (mA)	p (torr)	H_{max} (Gs)	I_{max} (mA)	H^2_{max}/I_o (Gs^2/mA)	$I_{max}p$ (mA torr)
3	0.1	175	0.45	10208	0.045
5	0.1	225	0.55	10125	0.055
8	0.1	235	0.90	6903	0.090
8	0.05	195	1.05	4753	0.053

Table 8

Variation of discharge current with magnetic field in CO_2 gas for a gas distance d = 3.5 cm

I_o (mA)	p (torr)	H_{max} (Gs)	I_{max} (mA)	H^2_{max}/I_o (Gs^2/mA)	$I_{max}p$ (mA torr)
3	0.20	165	0.2	9075	0.040
3	0.08	165	0.6	9075	0.048
3	0.05	165	0.7	9075	0.035
5	0.20	225	0.3	10125	0.06
5	0.08	235	0.75	11045	0.06
5	0.05	235	1.25	11045	0.06
8	0.20	200	0.60	5000	0.12
8	0.08	190	1.15	4513	0.09
8	0.05	260	1.80	8450	0.09

6.3 PLASMA PARAMETERS

Above the floating potential the probe current consists of two components: ion current and electron current. It is appropriate to plot only electron component against the probe potential, so ion saturation region is extended and the ion component is subtracted from the total current. Log i_e is plotted against the probe potential. For all gases, the probe characteristics corresponding to the currents of 4 and 7 mA do not show an appreciable linearity when the electron current is being increased. Hence, their probe characteristics are not analysed. Curves are plotted for the currents of 10,15 and 20 mA when the probe is at the axis (r = 0 mm) and at 10 mm (r = 10 mm) from the axis of the discharge tube.

Temperature of the electrons is calculated from the slope of the linear portion of the electron current and the Eqn. (4.42) is used for this purpose. The Eqn. (4.41) is used to calculate the telectron number density. The current corresponding to the intersection of tangents to linear portion and electron saturation portion is taken as electron saturation current. Some of the probe characteristics are shown in Figs. 26 to 29.

For every curve first the temperature is calculated. The electron mean free path λ_e is calculated for that temperature at a particular pressure. The mean free path in given by

$$\lambda_e = \frac{1}{pP_c} .$$

where P_c is the probability of collision.

Values of P_c are taken from 'Basic Data of Plasma Physics' (22). For example, the electron mean free path in argon is given in Table 9.

Electron saturation current density, J_{es}, at probe surface is given (as for determining n_e) by

$$(J_{es})_p = \frac{J_{es}}{1+\frac{3}{4}\left(\frac{r_p}{\lambda_e}\right)\ln\left(\frac{L}{r_p}\right)}$$

where $J_{es} = \frac{1}{4} n_e e\left(\frac{8kT_e}{m\pi}\right)^{1/2}$.

Temperature is calculated theoretically as follows :

We recall the Eqn. (3.17) :

$$\frac{e^x}{x^{1/2}} = 1.2\times10^7 (cpR)^2$$

where c is a constant dependent on the gas

p is pressure

R is the inner radius of the discharge tube

Table 9

Electron mean free path in argon for different electron temperatures (Ref. 22)

I	p = 0.5 torr		p = 1.0 torr	
mA	T_e eV	λ_e cm	T_e eV	λ_e cm
10	1.448	0.154	1.303	0.085
15	1.375	0.160	1.231	0.089
20	1.375	0.160	1.231	0.089

Similarly, λ_e's for p = 2.0 torr are also found.

$$x = \frac{eV_i}{kT_e}$$ (V_i - the ionization energy of the particular gas; T_e - electron temperature)

Here the constant c is calculated from the Eqn. (3.19)

$$c = \left(\frac{aV_i^{1/2}}{\mu_+}\right)$$

The mobility of positive ions, μ_+, at 1 torr is taken von Engel (1). The ionization potential V_i, and the constant are also given by von Engel. These values and the calculated values of c are tabulated in Table 10. The values of c are calculated only for argon and nitrogen because the constant a is not available for CO_2. Since positive column theory does not apply to oxygen and air, as they are electronegative gases, no attempt is made to calculate the temperature in these cases.

The value of x is calculated by successive approximation from which T_e is deduced and the radius of the tube is taken as R = 2.55 cm.

By determining the electron density at the axis of the tube with the probe, its values at a radial distance of 10 mm is theoretically calculated by the use of Eqn. (3.11).

Table 10

Calculated values of α for A and N_2

Gas	$ax10^2$ $volt^{-1}$	V_i eV	$\mu_+ \times 10^{-3}$ cm/sec per V/cm per torr	$cx10^{-2}$
A	71	15.755	1.2	4.065
N_2	26	15.58	2	3.900

In our case,

$$n_r = 0.689\ n_o$$

Cherrington (47) has given an expression relating discharge current and electron density at the axis of the tube for argon which is

$$I = 1.36\ n_{eo}(\mu_e)\ R^2 e \qquad (6.1)$$

μ_e is determined as given below :

Once the electron temperature is known, D/μ_e can be found by making use of Eqn. (3.2). The electron drift velocity corresponding to this D/μ_e is known from a reported (22) graph. At a given pressure, the field E can also be known from the same graph (22). When the drift velocity W and field E are known, μ_e can be easily calculated from the relationship

$W = \mu_e E$. Knowing R (= 2.55 cm) and the current I, the value of n_{eo} is calculated. As no such simple expression for nitrogen exists, no attempt is made to evaluate it in this case.

Theoretically calculated and experimentally determined values of plasma parameters (electron temperature and electron density) are given in Tables 11-20.

Table 11

Electron temperature and density in air*

	p = 0.2 torr		p = 0.5 torr	
I mA	T_e eV	$n_{eo} \times 10^{-10}$ cm^{-3}	T_e eV	$n_{eo} \times 10^{-10}$ cm^{-3}
10	1.74	0.63	1.59	1.60
15	1.67	0.72	1.52	2.53
20	1.67	1.21	1.52	4.46

Electron temperature and density in argon for p = 0.5 torr

I	r = 0 mm				r = 10 mm			
mA	T_e eV		n_{eo} $\times 10^{-10}$ cm^{-3}		T_e eV		n_{er} $\times 10^{-10}$ cm^{-3}	
	Expt	Theory	Expt	Theory Eqn.(6.1)	Expt	Theory	Expt	Theory Eqn.(3.11)
10	1.45	1.30	1.17	4.65	1.45	1.30	0.88	0.81
15	1.38	1.30	1.19	7.16	1.45	1.30	1.16	0.80
20	1.38	1.30	1.23	9.55	1.38	1.30	1.19	0.89

Table 13

Electron temperature and density in argon for p = 1 torr

I	r = 0 mm				r = 10 mm			
mA	T_e eV		n_{eo} $x10^{-10}$ cm^{-3}		T_e eV		n_{er} $x10^{-10}$ cm^{-3}	
	Expt	Theory	Expt	Theory	Expt	Theory	Expt	Theory
10	1.30	1.16	1.57	4.91	1.30	1.16	1.14	1.08
15	1.23	1.16	1.71	7.57	1.30	1.16	1.79	1.18
20	1.23	1.16	1.96	10.10	1.30	1.16	1.79	1.35

Table 14

Electron temperature and density in argon for p = 2 torr

I	r = 0 mm				r = 10 mm			
mA	T_e eV		n_{eo} $x10^{-10}cm^{-3}$		T_e eV		n_{er} $x10^{-10}cm^{-3}$	
	Expt	Theory	Expt	Theory	Expt	Theory	Expt	Theory
10	1.16	1.05	2.63	5.20	1.16	1.05	2.47	1.82
15	1.09	1.05	4.41	8.03	1.16	1.05	3.80	3.04
20	1.09	1.05	5.23	10.71	1.09	1.05	4.90	3.60

Table 15

Electron temperature and density in CO_2

I	p = 0.5 torr					p = 1 torr				
	r=0 mm		r=10 mm			r=0 mm		r=10 mm		
mA	T_e eV	n_{eo} $\times 10^{-10}$ cm^{-3}	T_e eV	n_{er} $\times 10^{-10}$ cm^{-3}		T_e eV	n_{eo} $\times 10^{-10}$ cm^{-3}	T_e eV	n_{er} $\times 10^{-10}$ cm^{-3}	
				Expt	Theory				Expt	Theory
10	1.38	0.70	1.38	0.31	0.48	1.30	1.48	1.30	1.14	1.00
15	1.38	1.48	1.45	0.85	1.02	1.30	3.04	1.23	1.38	2.10
20	1.38	1.70	1.38	0.98	1.17	1.23	3.44	1.23	1.19	2.38

Table 16

Electron temperature and density in nitrogen for p = 0.5 torr

I	r = 0 mm			r = 10 mm			
mA	T_e eV		n_{eo} x10^{-10} cm^{-3}	T_e		n_{er}x1 x10^{-10} cm^{-3}	
	Expt	Theory		Expt	Theory	Expt	Theory
10	1.38	1.29	1.25	1.38	1.29	1.14	0.86
15	1.38	1.29	2.19	1.38	1.29	1.72	1.51
20	1.30	1.29	2.61	1.30	1.29	2.77	1.80

Table 17

Electron temperature and density in nitrogen for p = 1 torr

I	r = 0 mm			r = 10 mm			
mA	T_e eV		n_{eo} $\times 10^{-10}$ cm^{-3}	T_e eV		n_{er} $\times 10^{-10}$ cm^{-3}	
	Expt	Theory		Expt	Theory	Expt	Theory
10	1.23	1.15	3.23	1.23	1.15	2.07	2.22
15	1.23	1.15	4.15	1.23	1.15	3.92	2.86
20	1.23	1.15	5.76	1.23	1.15	5.99	3.97

Table 18

Electron temperature and density in oxygen for p = 0.2 torr

	r = 0 mm		r = 10 mm		
nA	T_e eV	n_{eo} x10^{-10}cm^{-3}	T_e eV	n_{er} x10^{-10}cm^{-3}	
				Expt	Theory
10	1.52	0.66	1.52	0.45	0.45
15	1.52	2.23	1.52	1.07	1.53
20	1.52	4.72	1.45	3.10	3.25

Table 19

Electron temperature and density in oxygen for p = 0.5 torr

I	r = 0 mm		r = 10 mm		
mA	T_e eV	n_{eo} x10^{-10}cm^{-3}	T_e eV	n_{er} x10^{-10}cm^{-3}	
				Expt	Theory
10	1.23	3.33	1.23	1.47	2.30
15	1.23	3.83	1.23	3.70	2.64
20	1.23	8.64	1.23	4.32	5.95

Table 20

Electron temperature and density in oxygen for p = 1 torr

iA	r = 0 mm		r = 10 mm		
	T_e eV	n_{eo} x10^{-10}cm^{-3}	T_e eV	n_{er} x10^{-10}cm^{-3}	
				Expt	Theory
10	1.16	5.11	1.16	4.60	3.52
15	1.09	6.68	1.09	7.21	4.60
20	1.09	14.06	1.09	7.21	9.69

The results are discussed in the next chapter.

CHAPTER 7

DISCUSSION AND CONCLUSIONS

7.1 COLLISION FREQUENCY

The Paschen curves show a qualitative agreement with the observation of earlier workers. For all gases, the collision frequencies vary with E/p and H/p. As Tables 1-6 show, for the same breakdown potential, the collision frequency increases with H/p while H is low, and for higher values (1000-3000 Gs) it becomes constant. It is also seen that, when a set of breakdown potentials for both low and high magnetic fields is taken into account, the collision frequency decreases with E/p and H/p. The p^2 vs H^2 curves for argon show a sharp bend between low and high magnetic fields. Such an observation has not been reported earlier. Before making any comment on this observation, it is necessary that the experiment should be carried out for a range of H between 0-1000 Gs.

Dargan and Heylen (14) have reported a constant value of $\nu_o = 3\times10^9$ (storr)$^{-1}$ for hydrogen for 30 < E/p < 110 V cm^{-1}torr^{-1}. The values of ν_6 in our case, varying between $3.11\text{-}4.27\times10^9$(storr)$^{-1}$, are quite comparable with this value when H is high (Table 4). For low H, for a specific breakdown potential, the collision frequency varies between 1.0 and

2.0×10^9 $(\text{storr})^{-1}$ as seen from Table 4. As pointed out by Haydon (15), it is appropriate to discuss the variation of collision frequency as a function of E/p' rather than E/p and H/p, where p' is the equivalent pressure. Such a variation of ν_o with E/p' cannot be established from breakdown voltage measurements alone. It requires pre-breakdown measurements also.

For nitrogen, earlier workers have reported a constant value of ν_o at 8×10^9 $(\text{s torr})^{-1}$ when E/p lies in the range $150 < E/p < 200$ V cm^{-1} torr^{-1}. In this work it is 7.9×10^9 $(\text{storr})^{-1}$ for an E/p of 162 V cm^{-1} torr^{-1} and it reaches a value of 5.3×10^9 $(\text{storr})^{-1}$ at an E/p of 113 V cm^{-1} torr^{-1}. It is to be mentioned that for all gases done in this experiment, the collision frequencies calculated for high magnetic fields, that is low slope parts of p^2 vs H^2 plots, nearly coincide with the values reported earlier. This is found to be true for all gases.

Such work for oxygen has not been reported so far so there are no data to compare the results obtained in this experiment, in which the collision frequency is calculated as 9.5×10^9 $(\text{storr})^{-1}$ at an E/p of 236 V cm^{-1} torr^{-1} and 7.8×10^9 $(\text{storr})^{-1}$ at an E/p of 66 $(\text{storr})^{-1}$.

For CO_2 also, collision frequencies are not reported earlier. In this experiment, ν_o is obtained as high as

27.9×10^9 $(\text{storr})^{-1}$ when E/p = 348 V $cm^{-1}/torr^{-1}$ and H/p = 435 Gs $torr^{-1}$. And it is 11.5×10^9 $(\text{storr})^{-1}$ for on E/p of 674 V cm^{-1} $torr^{-1}$ and H/p of 2247 $Gstorr^{-1}$. The variation of ν_o is seen in Table 3.

For argon, ν_o varies from 4.1×10^9 $(\text{storr})^{-1}$ to 6×10^9 $(\text{storr})^{-1}$ for a wide range of E/p and H/p. The steep rise of the p^2 vs H^2 plots at low magnetic fields for argon cannot be reliable because it gives very low values of ν_o as 0.48×10^9 $(\text{storr})^{-1}$, whereas the reported value is 4.1×10^9 $(\text{storr})^{-1}$. The p^2 vs H^2 curve for larger values of H^2 if represented by a straight line approximation it gives values for ν_o, in agreement with the reported value in the literature.

For air, this work shows higher values of collision frequency than the reported value. A value of $4.4 \times 10^9 (\text{storr})^{-1}$ is reported for E/p = 212 V cm^{-1} $torr^{-1}$ and H/p = 108 Gs $torr^{-1}$, whereas the present work gives 6.9×10^9 $(\text{storr})^{-1}$.

In conclusion varies with E/p and H/p. For small range of these values, ν_o is found to be constant, but generally ν_o decreases with E/p and H/p. Because of many underlying assumptions in the EPC and the errors in measurements, the collision frequencies cannot be accurate. But it should be stated that better results can be obtained if the variation of the secondary Townsend coefficient, γ, is studied through pre-breakdown measurements. A new approach-equivalent reduced electric field

concept - has been proposed by Heylen and Bunting (40) and substantiated by Heylen (41). This concept also provides the information regarding the collision frequency.

7.2 VARIATION OF DISCHARGE CURRENT IN MAGNETIC FIELD

As seen from Figs. 24 and 25, the discharge current increases with the magnetic field and reaches a minimum, and then gradually decreases. This phenomenon can be explained as follows.

The magnetic fields deflects the electrons and ions from the axis of the cylindrical plasma and pushes them towards the wall, thereby increasing the loss of electrons and ions. In order to compensate for this loss, it has been shown by Beckman that the axial electric field increases, thus increasing the ionization and electron temperature. Now more charged particles are produced, and hence a higher current. But for higher electric fields, the rate of ionization reaches a saturation, and so the loss at higher magnetic fields is not compensated for by the production of charged particles. This causes the decrease in discharge current. At still higher magnetic fields, the loss is so high that the discharge is extinguished.

Since no data on the fractional loss of energy of electrons is available for CO_2, no attempt is made to calculate the electron temperature from H_{max} using the Eqn. (4.35).

The values of H_{max}, I_{max} are reported in Tables 7 and 8. Also calculated are H^2_{max}/I_o and $I_{max}p$, which are given in the tables. For the d of 0.5 cm, it is found that for a specific starting current H^2_{max}/I_o and $I_{max}p$ are not constant as reported earlier (33). But for the gap distance of 3.5 cm, for a specific starting current $I_{max}p$ is nearly constant. The quantity H^2_{max}/I_o is constant for the starting current of 3 mA; for 5 mA, at pressures of 0.08 torr and 0.05 torr, this quantity is constant in agreement with the conclusion arrived at by Sen and Gupta (33); but that corresponding to the pressure of 0.2 torr, it slightly deviates. For the starting current of 8 mA, for various pressures, no constancy of H^2_{max}/I_o is obtained. They vary within a factor of 1.5.

7.3 PLASMA PARAMETERS

The experimental and calculated values of electron temperature and density for various gases are tabulated from Tables 11 to 20. Owing to many assumptions underlying in the theories of both positive column and probe, it is not simple to explain the deviations of one from the other.

Regarding the electron temperature, the general observation in argon and nitrogen is that the experimental values are slightly greater than the theoretical values, for all currents and pressures. At least one concept of the positive column is justified here: as pressure is increased, the

elcctron temperature decreases for all the gases considered. According to the positive column theory, the electron temperature does not depend on the discharge current. Though in a few instances it is so, higher currents show lower electron temperatures. Also, the radial variation of electron temperature is observed. Since there is no particular consistency in this variation, the cause may be attributed to error in measurements of current and voltage.

Regarding the electron density, the results in argon show that the experimental values are much less than the calculated values. This discrepancy may be attributed to the uncertainty in locating the plasma potential. The density at the radial position of 10 mm from the axis show large deviations from those calculated from theory (assuming the experimental values for n_{eo}) except for a few cases. It may be concluded that a better way of locating the plasma potential is sought for better density results. In these preliminary experiments the probe does yield at least the order of magnitude for the density. It is clear from the results that the experimental values are in good agreement with the theory.

In conclusion, the collision frequencies obtained are reasonably accurate. Better results can be obtained by doing pre-breakdown measurements with accurate measuring equipments. Probe also gives accurate temperature results and with lesser accuracy the density results.

9. Cummings et al., 'Influence of Longitudinal Magnetic Field on an Electric Discharge in Mercury Vapour at Low Pressure', Phys. Rev. 59, 514 (1941).

10. Beckman, L., 'The Influence of a Transverse Magnetic Field on a Cylindrical Plasma', Proc. Phys. Soc. 61, 515 (1948).

11. Heylen, A.E.D., 'The Influence of a Crossed Magnetic Field on a Gaseous Townsend Discharge', Brit. J. Appl. Phys. 16, 1151 (1965).

12. Townsend, J., and Gill, 'Generalization of the Theory of Electrical Discharges', Phil.Mag. 26, 290 (1938).

13. Blevin, H.A., and Haydon, S.C., 'The Townsend Ionization Coefficients in Crossed Electric and Magnetic Fields', Aust. J. Phys. 11, 18 (1958).

14. Dargan, C.L., and Heylen, A.E.D., 'Uniform-field Sparking Voltages of Gases in Crossed Magnetic Fields', Proc. IEE, 115, 1034 (1968).

15. Haydon, S.C., 'Critical Comparison of Methods for the Evaluation of Electron-Molecule Collision Frequencies in Crossed E and H Fields', Proc. IEE 117, 473 (1970).

16. Guharay, S.K., and Sen Gupta, S.N., 'Effect of a Transverse Magnetic Field on the Sparking Characteristics of Gases at Low Pressures', Indian J. Phys. 50, 9 (1976).

17. Sengupta, D., et al., 'Electron Neutral Collision Frequency from Breakdown Measurements in Crossed Electric and Magnetic Fields', Pramana 11, 661 (1978).

18. Langmuir, I., and Mott-Smith, H., 'Studies of Electrical Discharges in Gases at Low Pressures, Part I-V', Gen. Elec. Rev. 27, 449,538,616,762,810 (1924).

19. Meek, J.M. and Craggs, I.D., Electrical Breakdown of Gases, John Wiley and Sons, Chichester (1978).

20. Nasser, E., Fundamentals of Gaseous Ionization and Plasma Electronics, John Wiley and Sons, New York (1971).

21. Huxley, L.H., and Crompton, R.W., The Diffusion and Drift of Electronics in Gases, John Wiley and Sons, New York (1974).

22. Brown, S.C., Basic Data of Plasma Physics, MIT Press and John Wiley and Sons (1959).

23. Waters, R.T., 'Diagnostic Techniques for Discharges in Gases', in Electrical Breakdown and Discharges in Gases (Eds. E.E. Kunhardt and L.H. Luessen), Plenum Press, New York (1983).

24. Bastien, F., 'Spectroscopic Diagnostics in Gas Discharges', in Electrical Breakdown and Discharges in Gases (Eds. E.E. Kunhardt and L.H. Luessen),

25. Balaraman, S., Plasma References (Published Works upto 1983), NETP, IIT Kanpur (1983).

26. Bernstein, N.J., 'Electron Drift and Diffusion Measurements in H_2 and D_2 with Crossed Electric and Strong Magnetic Fields', Phys. Rev. 127, 335 (1962).

27. Fletcher, J., and Haydon, S.C., 'Transport and Ionization Properties of Molecular Gases in a Transverse Magnetic Field', Aust. J. Phys. 19, 615 (1966).

28. Heylen, A.E.D., and Dargan, C.L., 'Calculated Magnetic Electron Drift Velocities in H_2, N_2, O_2, air, and C_2H_6 for $10 \leq E/p \leq 10^4$ $Vcm^{-1}torr^{-1}$', Brit. J. Appl. Phys. 17, 1075 (1966).

29. Gurumurthy, G.R., and Govinda Raju, G.R., 'Townsend's First Ionization Coefficients and Sparking Potentials in Crossed Electric and Magnetic Fields', IEEE Trans. Plasma Sci. PS-3, 131 (1975).

30. Haydon, S.C., and Robatson, J., 'The Effective Collision Frequency in Molecular Hydrogen in the Presence of a Transverse Magnetic Field', Proc. Phys. Soc. 82, 343 (1963).

31. Bhiday, M.R. et al, 'Measurement of α/p for Air in Transverse Electric and Magnetic Fields', J.Phys. D 3, 943 (1970).

32. Somerville, 'Sparking Potentials in a Transverse Magnetic Field', Proc. Phys. Soc. 65, 620 (1952).

33. Sen, S.N., and Gupta, R.N., 'Variation of a Discharge Current in a Transverse Magnetic Field in a Glow Discharge', J.Phys. D 4, 510 (1971).

34. Chao, K.T., 'Electron Temperatures in Electrical Discharges', Phys. Rev. 68, 30 (1945).

35. Schulz, G.J., and Brown, S.C., 'Microwave Study of Positive Ion Collection by Probes', Phys. Rev. 98, 1642 (1955).

36. Okuda and Yamamoto, 'A New Probe Method for Measuring Ionized Gases', J.Phys. Soc. Jap. 13, 411 (1958).

37. Zakharova, V.M. et al, 'Probe Measurements at Medium Pressures', Sov. Phys. Tech. Phys. 5,411(1960).

38. Cellarius, C.J. et al, 'Determination of the Densities and Temperatures of Two Low Electron Energy Groups in a Hollow Cathode Discharge', Z. Physik. 231, 119 (1970).

39. Johnson, E.O. and Malter, L., 'A Floating Double Probe Method for Measurement in Gas Discharges', Phys.Rev. 80, 58 (1950).

40. Haylen, A.E.D., and Bunting, K.A., 'Electron Drift Velocities in a Moderate and in a Strong Crossed Magnetic Field', Int.J. Electron. 27, 1 (1969).

41. Heylen, A.E.D., 'Interpretation and Prediction of Gaseous Electrical-Breakdown Characteristics in a Crossed Magnetic Field', Proc. IEE 126, 215 (1979).

APPENDIX

SOME IMPORTANT COLLISION PROCESSES

(1)	$e+X$	$X^{*}+e$	collisional excitation
(2)	$e+X^{*}$	$X+e$	superelastic collision
(3)	$e+X$	$X^{+}+e+e$	collisional ionization
	$e+X^{*}$	$X^{+}+e+e$	
(4)	$X^{+}+e+e$	$X+e$	collisional recombination
(5)	$e+XY$	$e+X+Y$	dissociation
(6)	$e+YZ^{+}$	$Y+Z^{*}$	dissociative recombination
(7)	$e+X$	$X^{-}+h\nu$	radiative attachment
(8)	$X^{-}+h\nu$	$e+X$	photo-detachment
(9)	$X+Y^{+}$	$X^{+}+Y$	charge transfer
(10)	$X^{*}+Z$	$X+Z^{+}+e$	Penning ionization

X,Y,Z are atoms or molecules

X^{*} represents X is excited

e is electron .

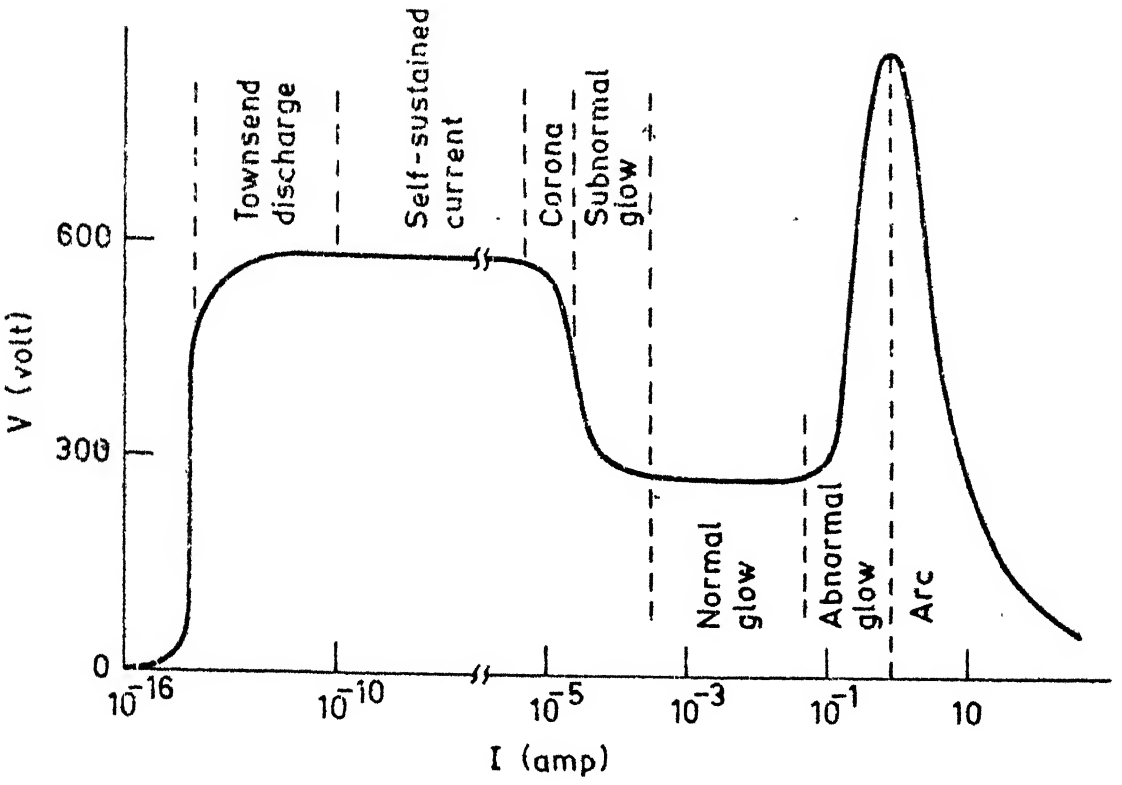

Fig. 1. Classification of discharge.

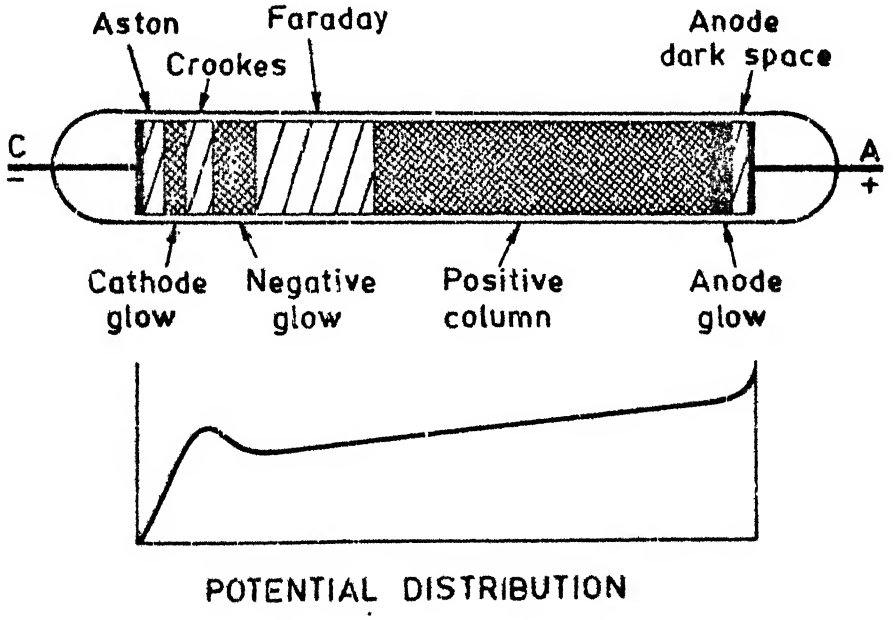

Fig. 2. Classification of glow discharge.

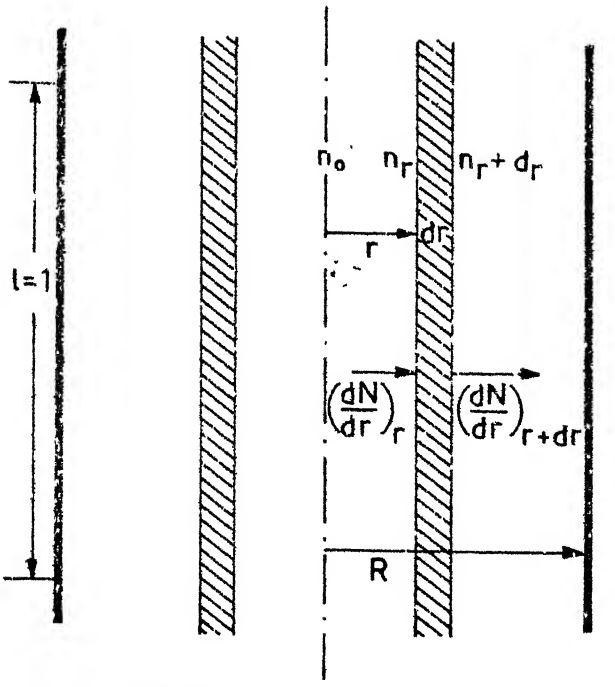

Fig. 3. To derive the radial distribution of charges.

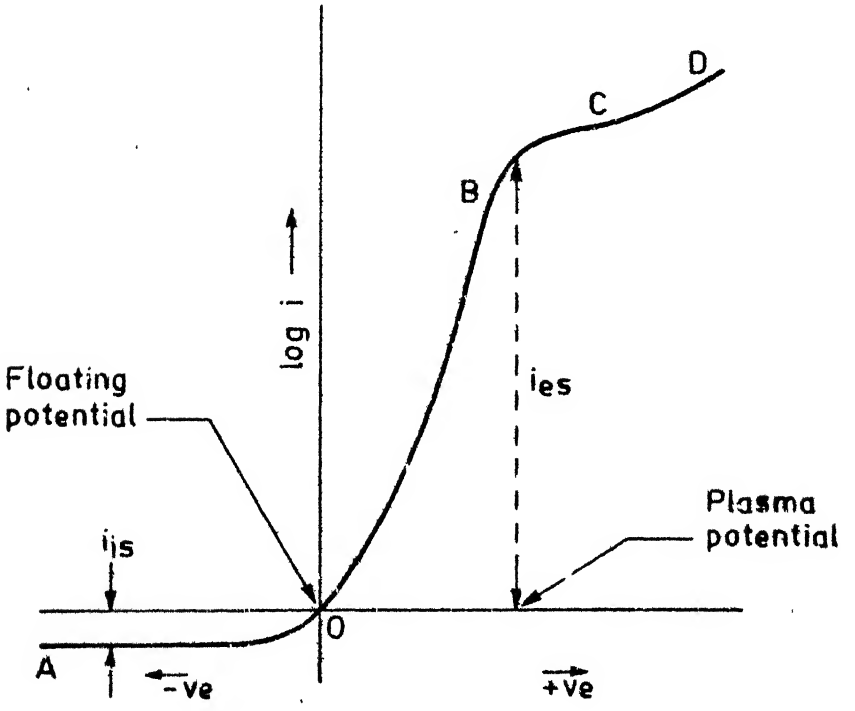

Fig. 4. Langmuir probe characteristic.

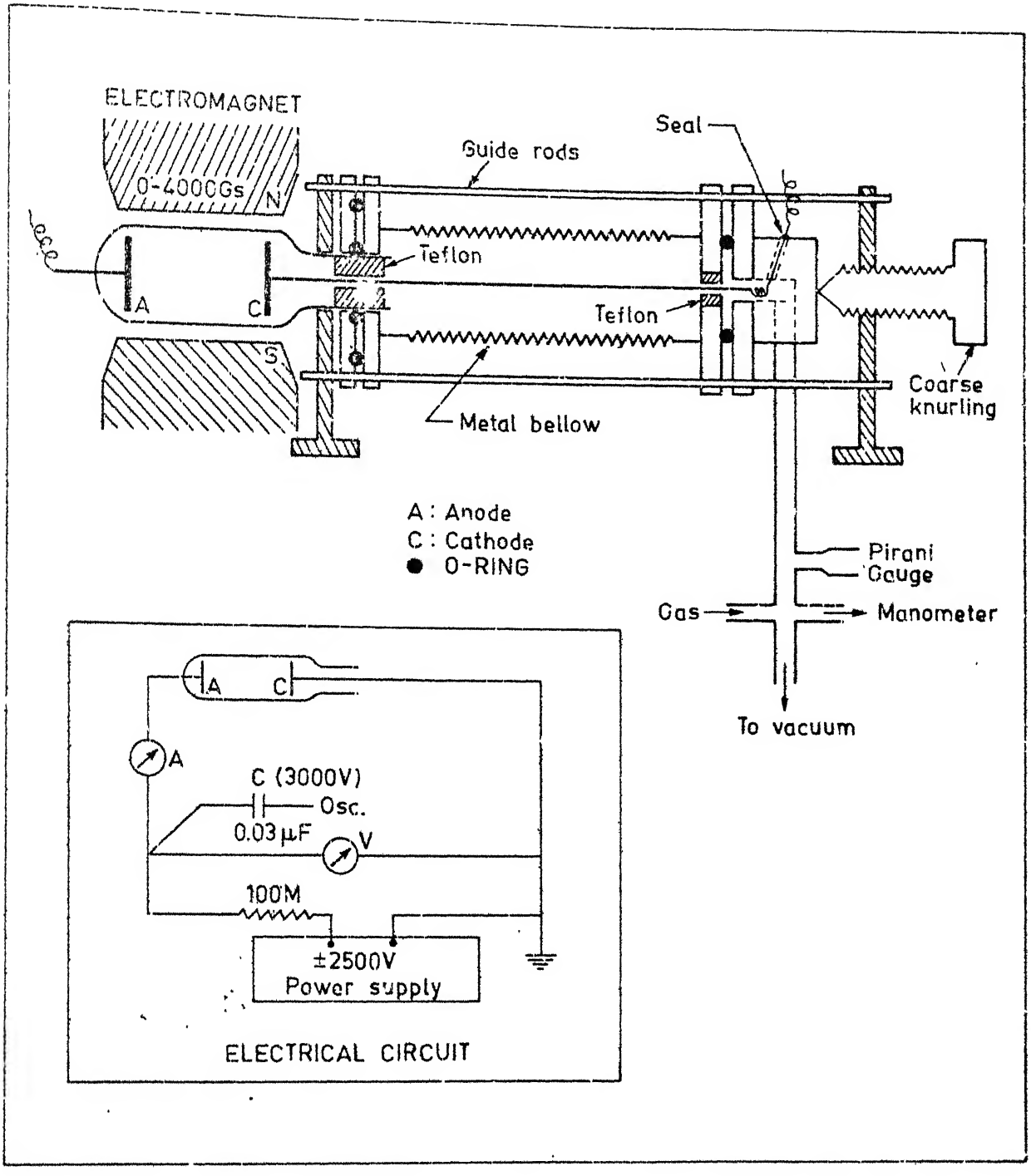

Fig. 5. Schematic diagram of experimental arrangement to study discharge characteristics in magnetic field.

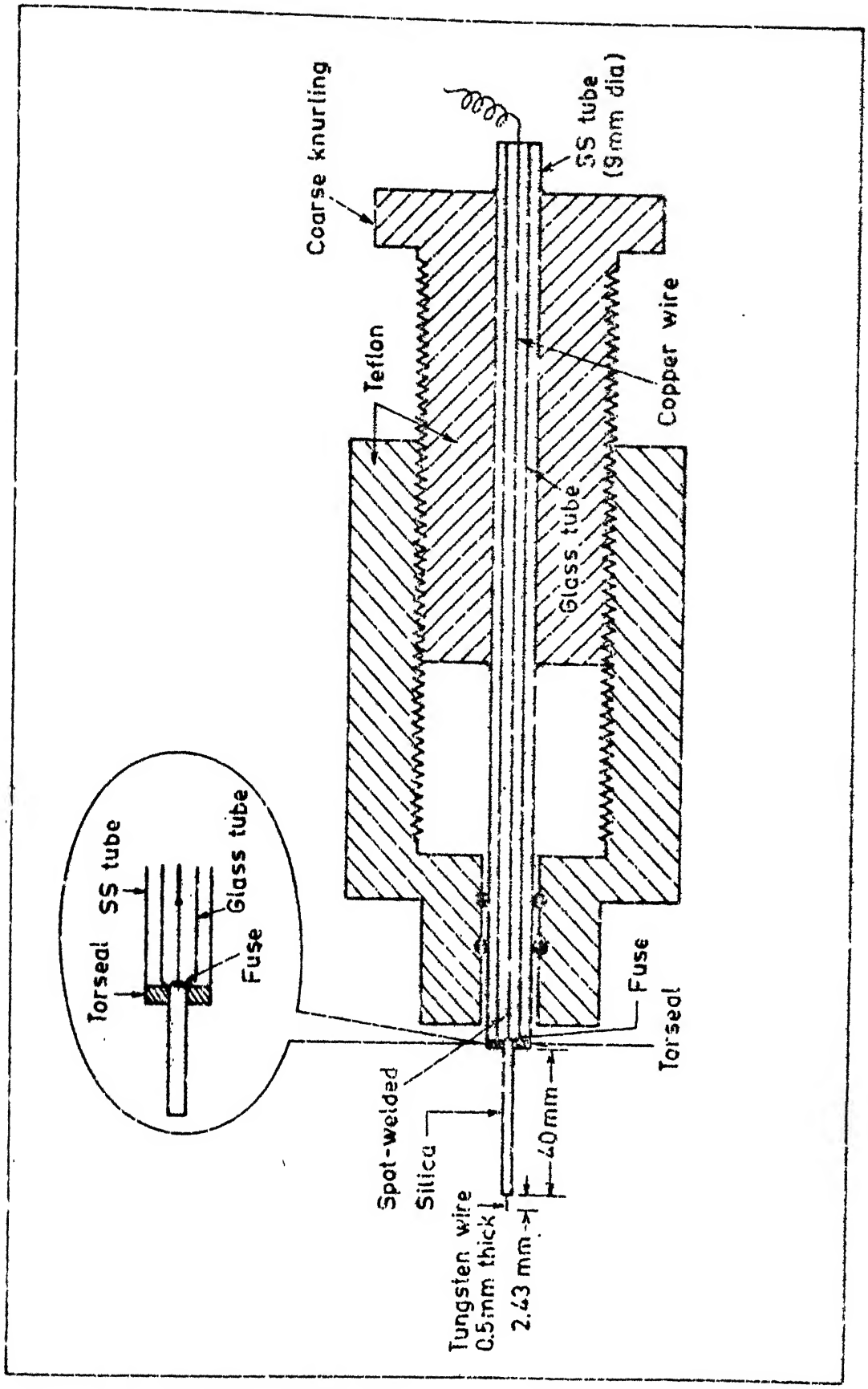

Fig. 6. Langmuir probe.

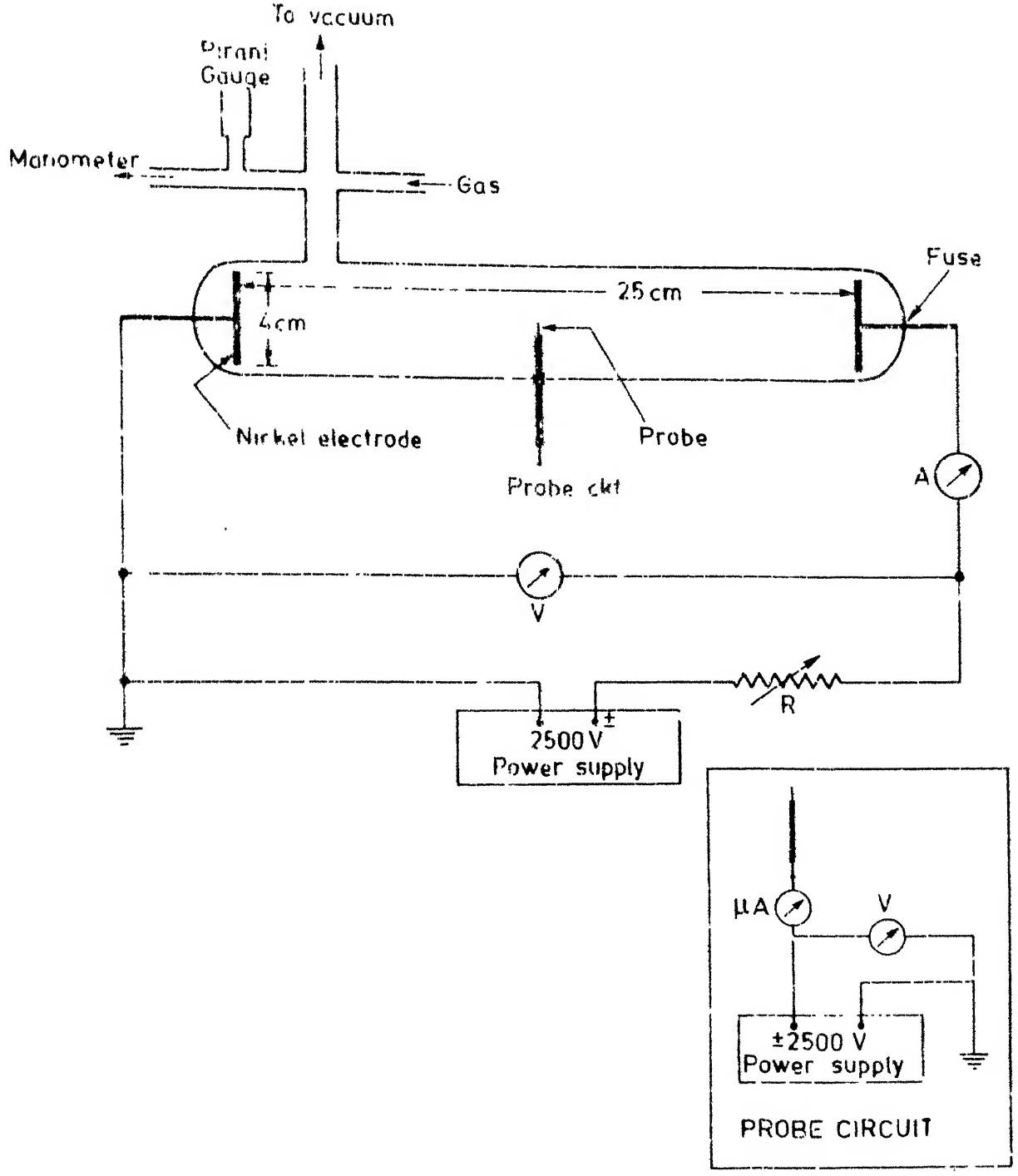

Fig. 7. Discharge tube and Langmuir probe.

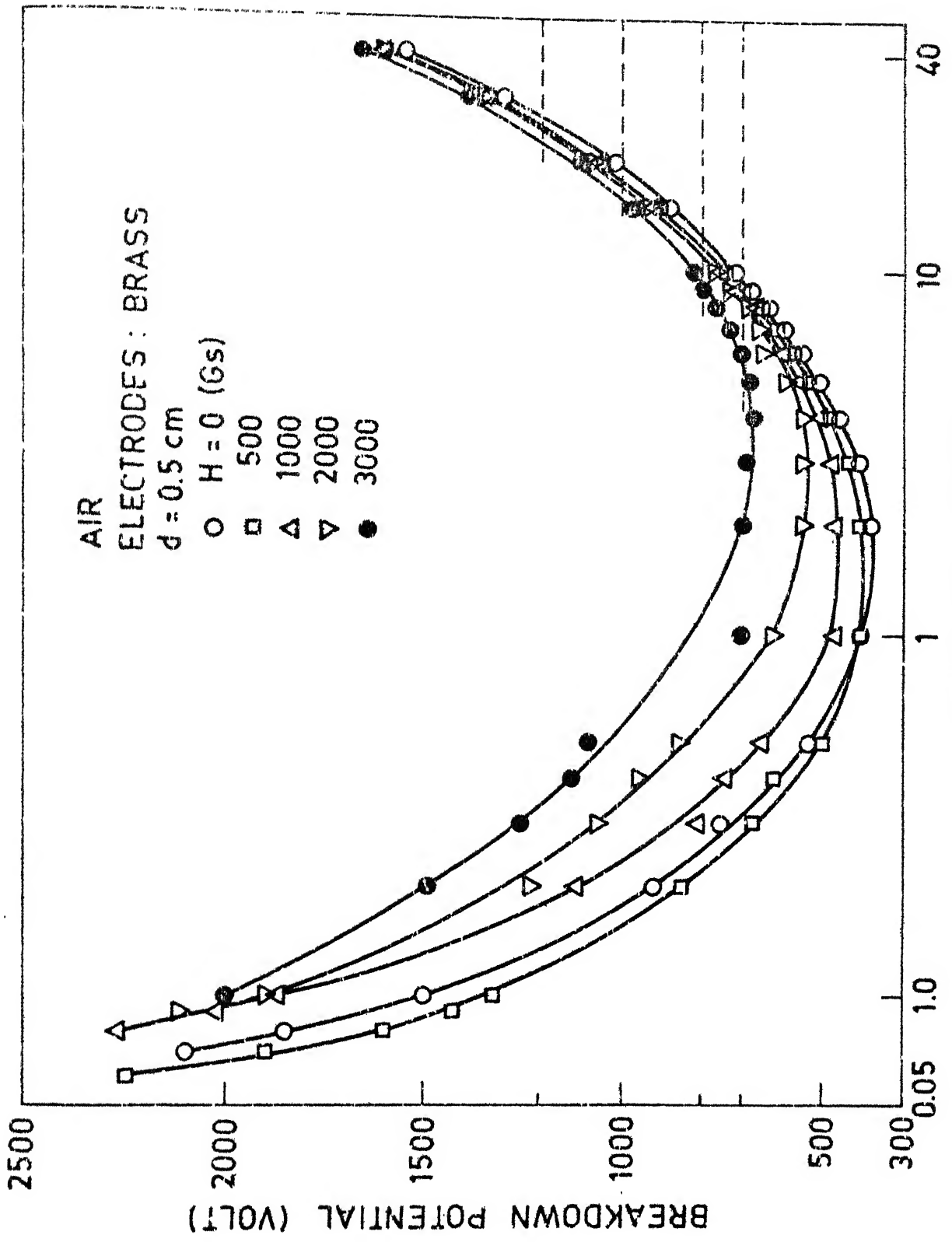

Fig. 8. Sparking voltage characteristics for air. d=0.5 cm.

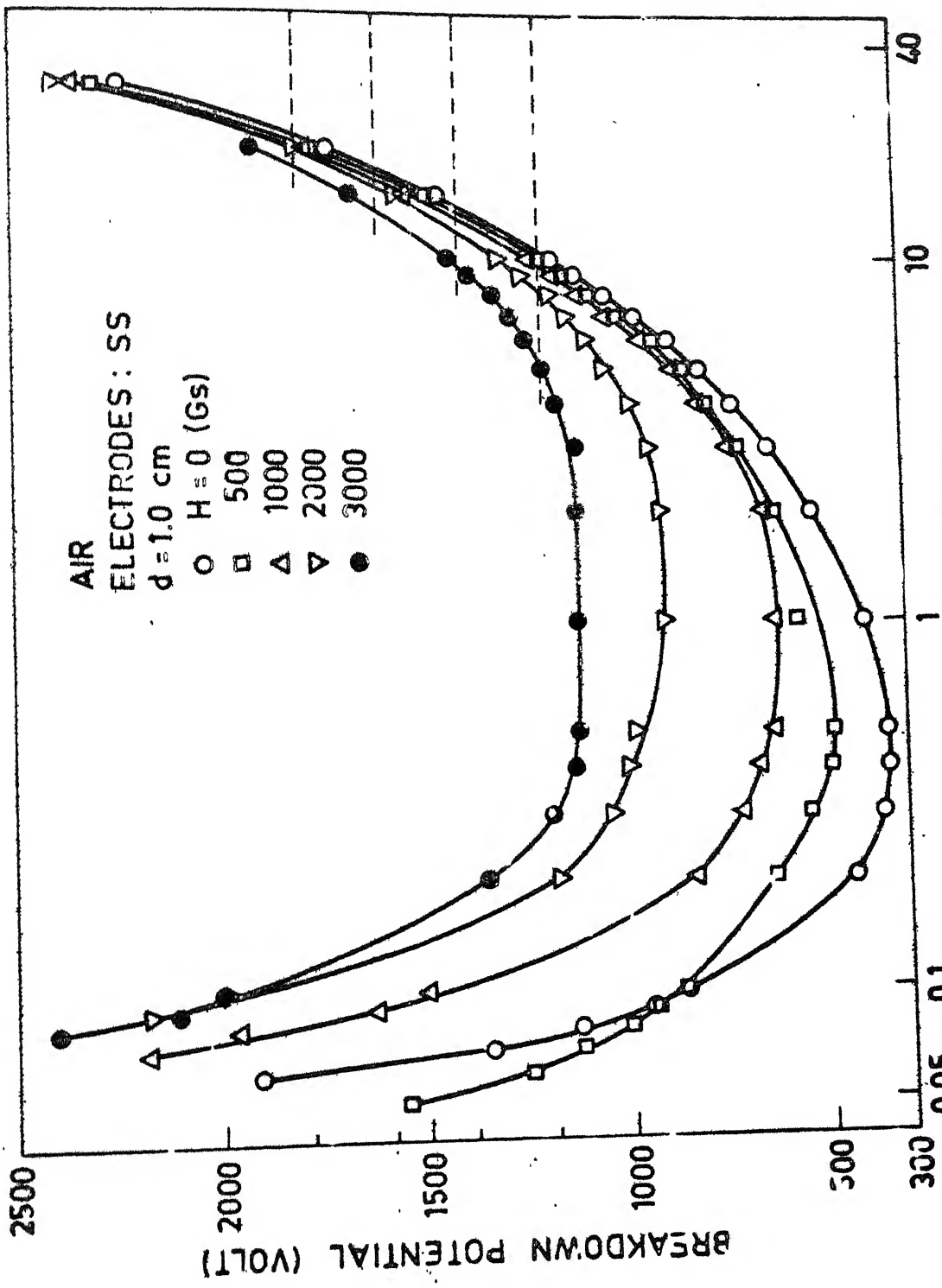

Fig. 9. Sparking voltage characteristics for air. d = 1.0 cm

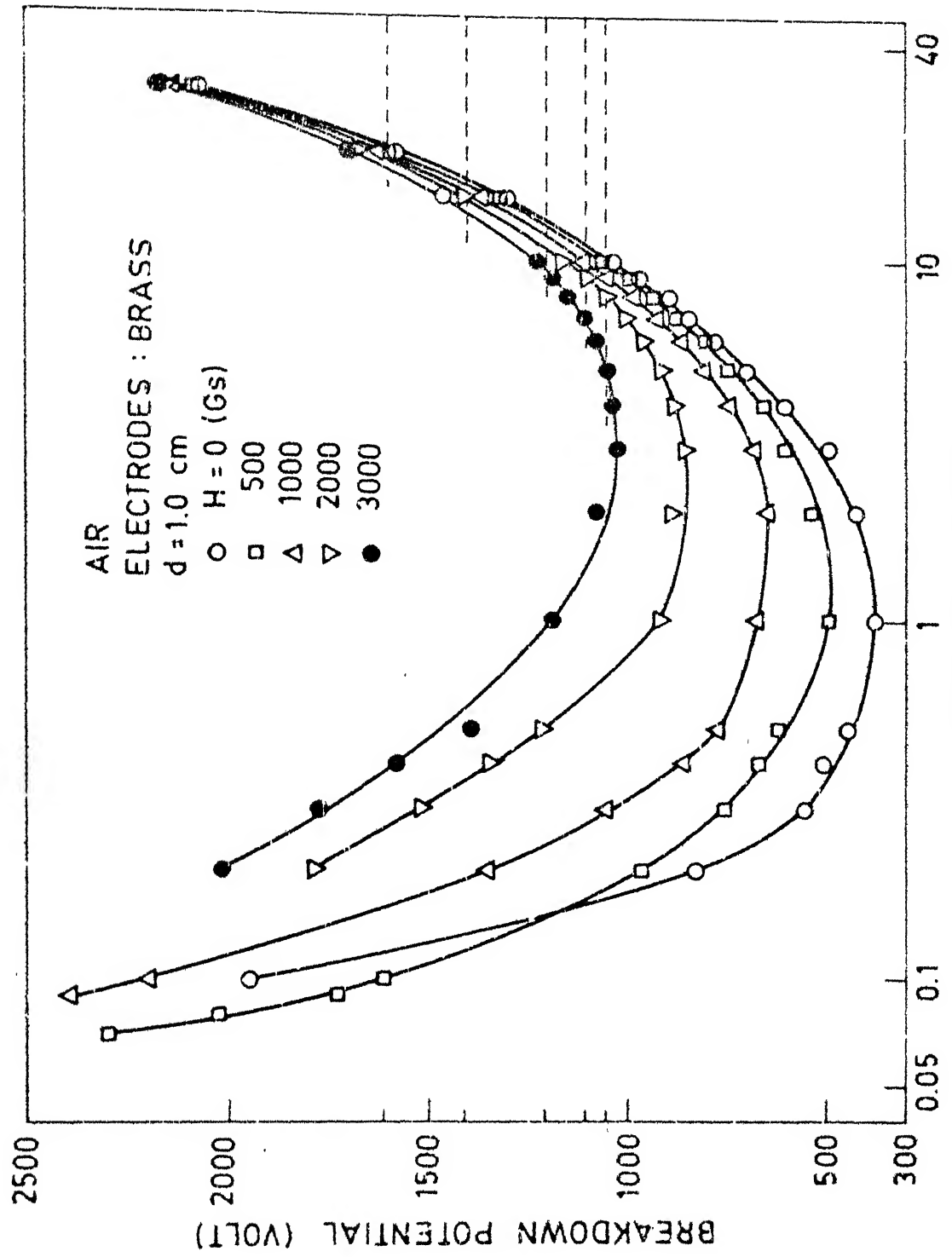

Fig. 10. Sparking voltage characteristics for air. d = 1.0 cm.

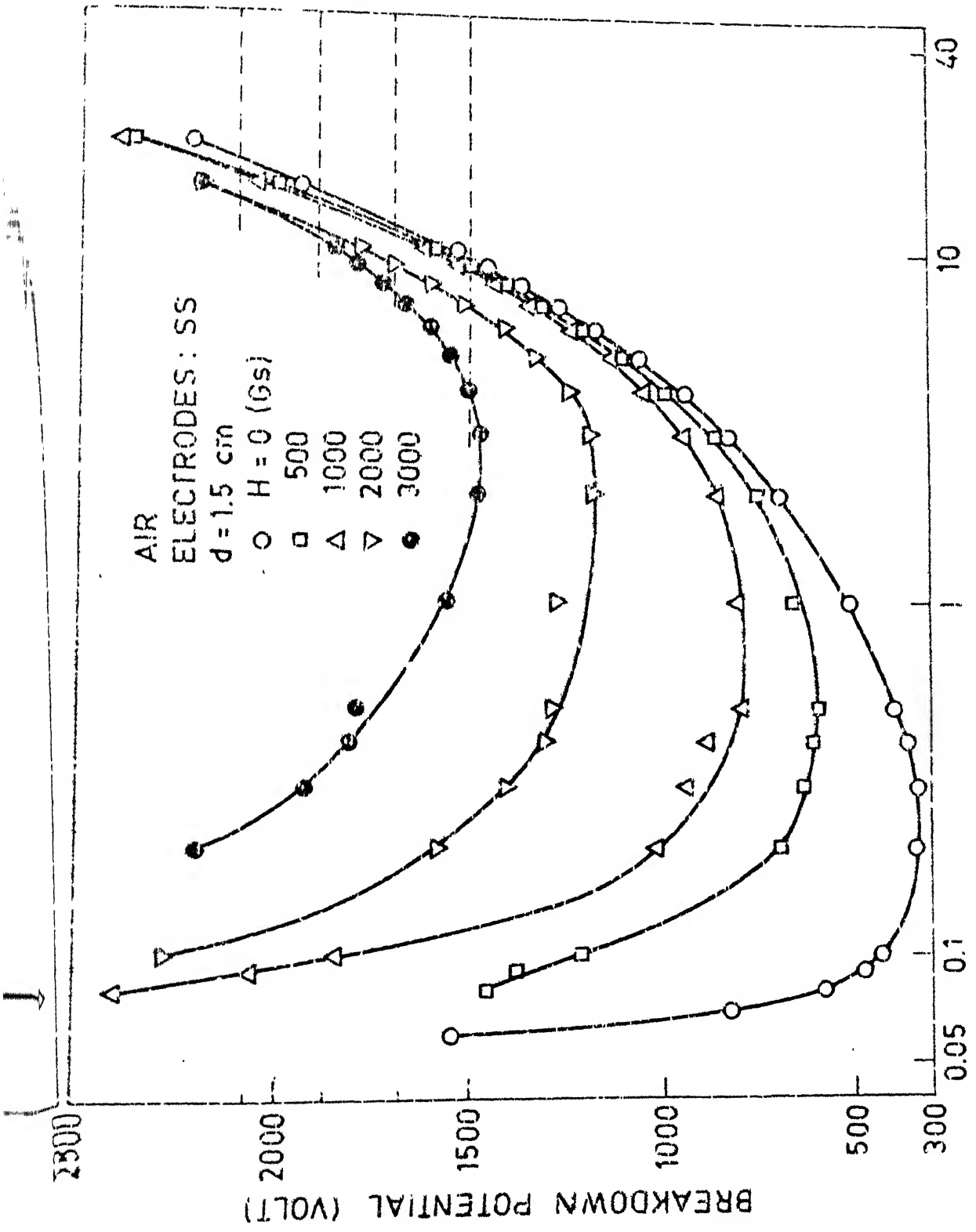

Fig. 11. Sparking voltage characteristics for air. d=1.5 cm.

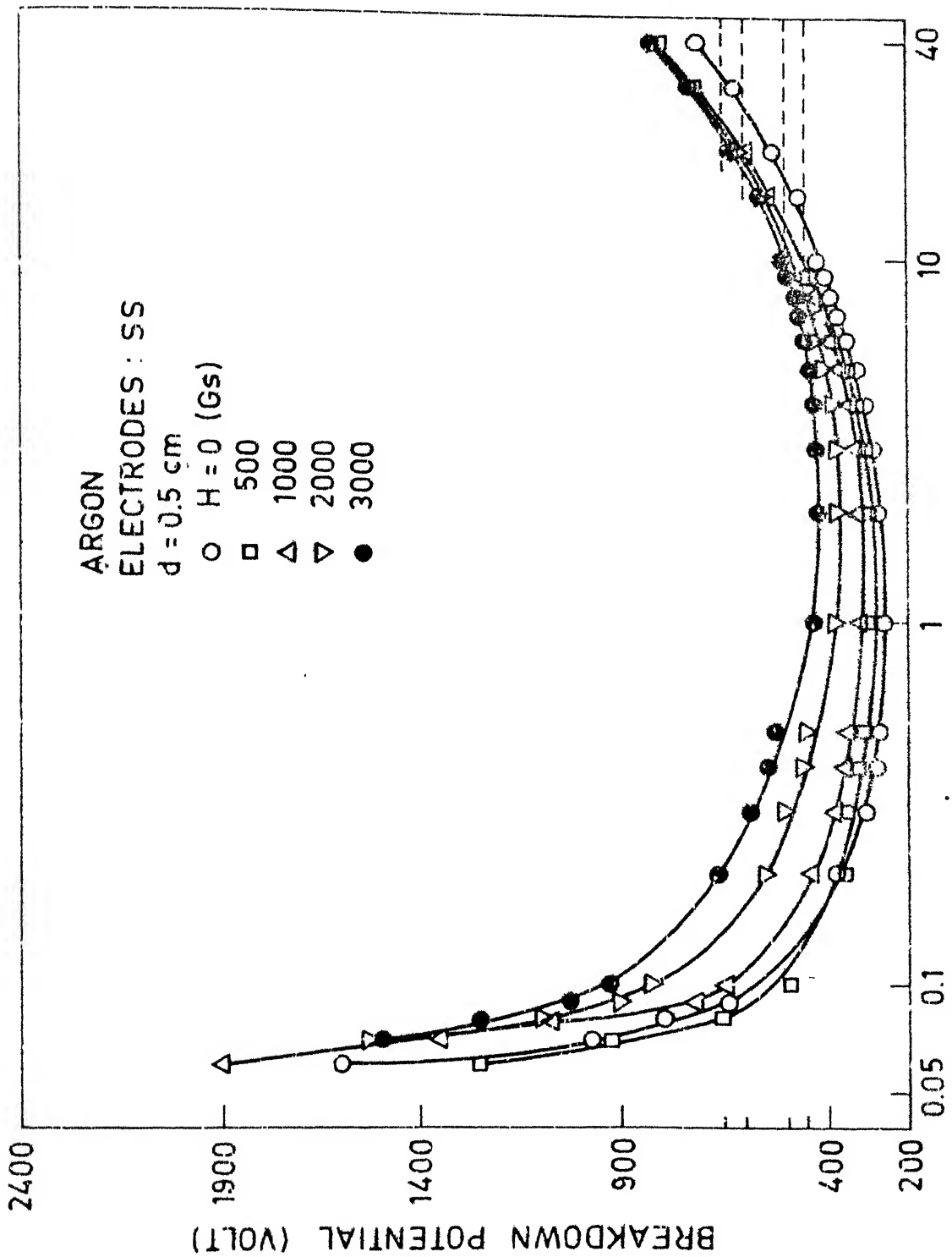

Fig. 12. Sparking voltage characteristics for argon. d=0.5 cm.

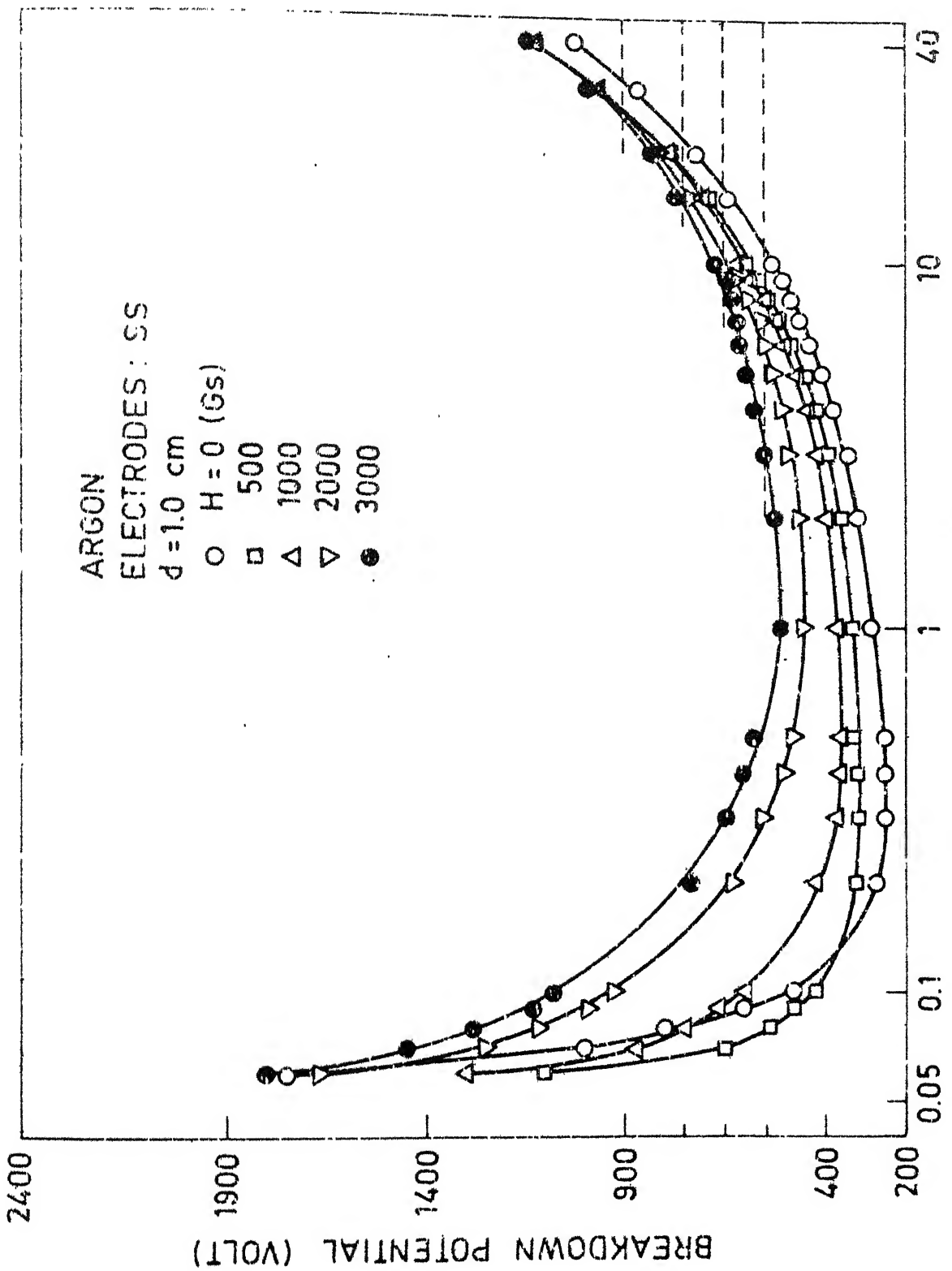

Fig. 13. Sparking voltage characteristics for argon. d = 1.0 cm.

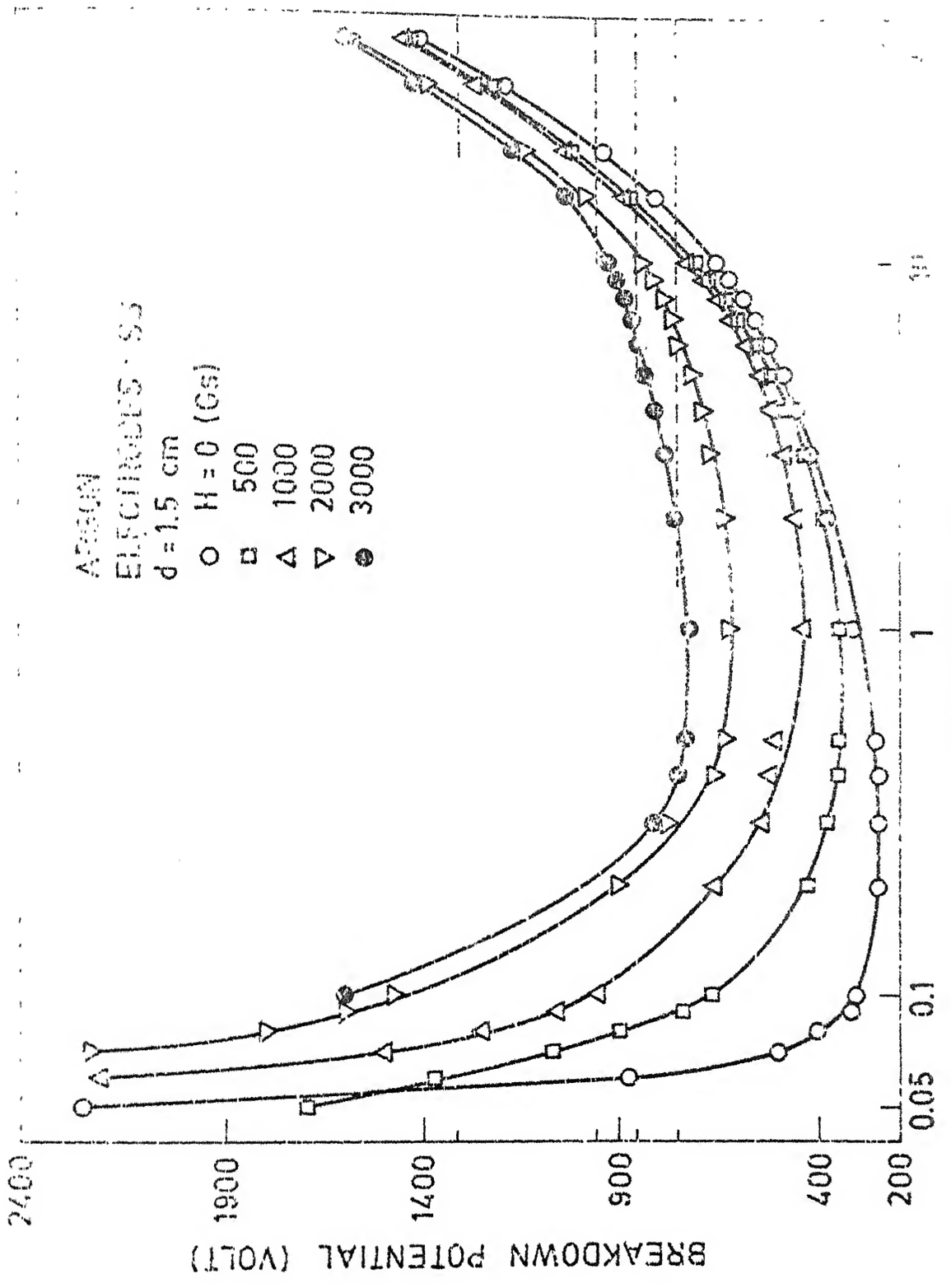

Fig. 14. Sparking voltage [illegible]

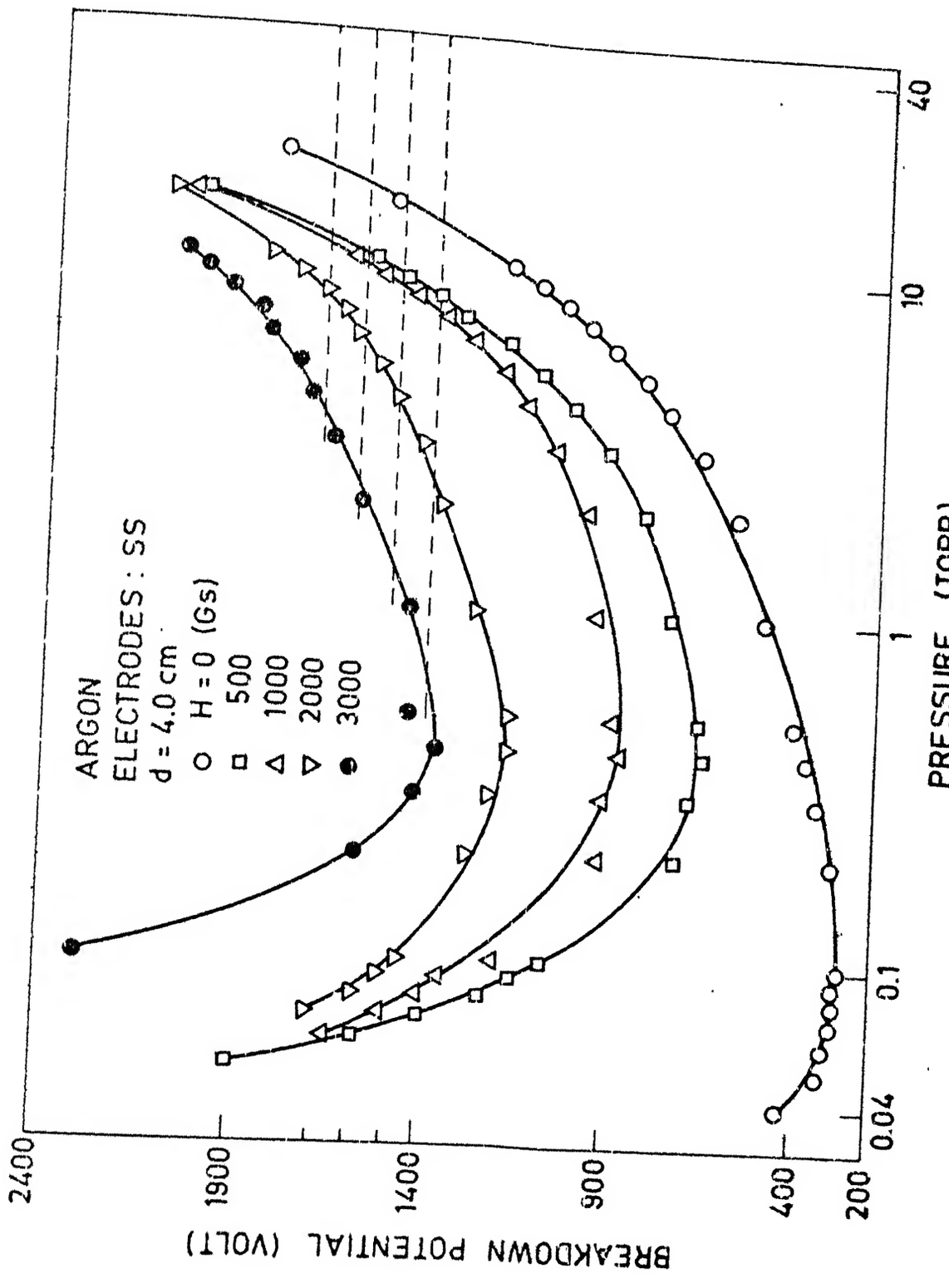

Fig. 15. Sparking voltage characteristics for argon. d = 4.0 cm.

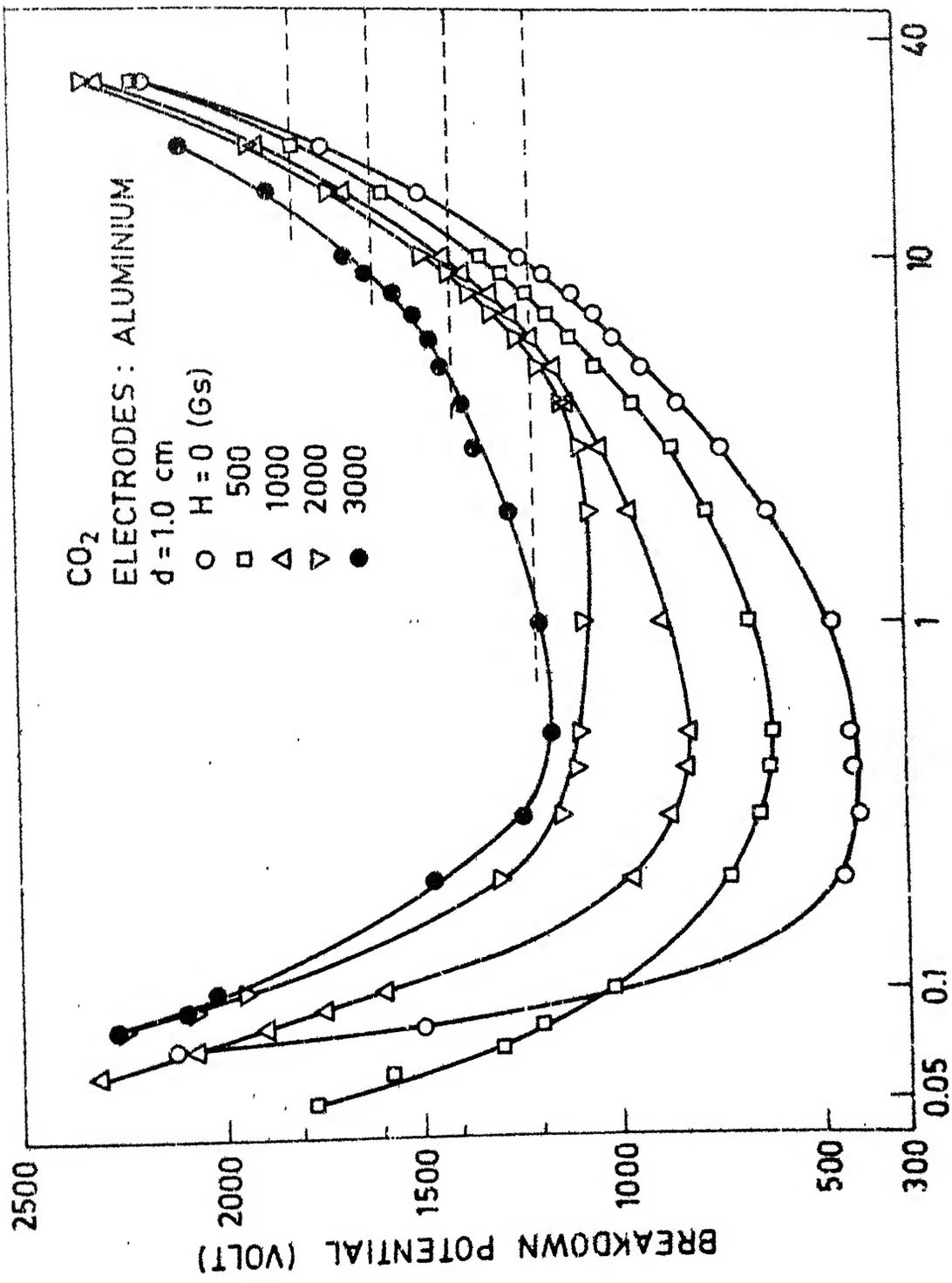

Fig. 16. Sparking voltage characteristics for CO_2. d = 1.0 cm.

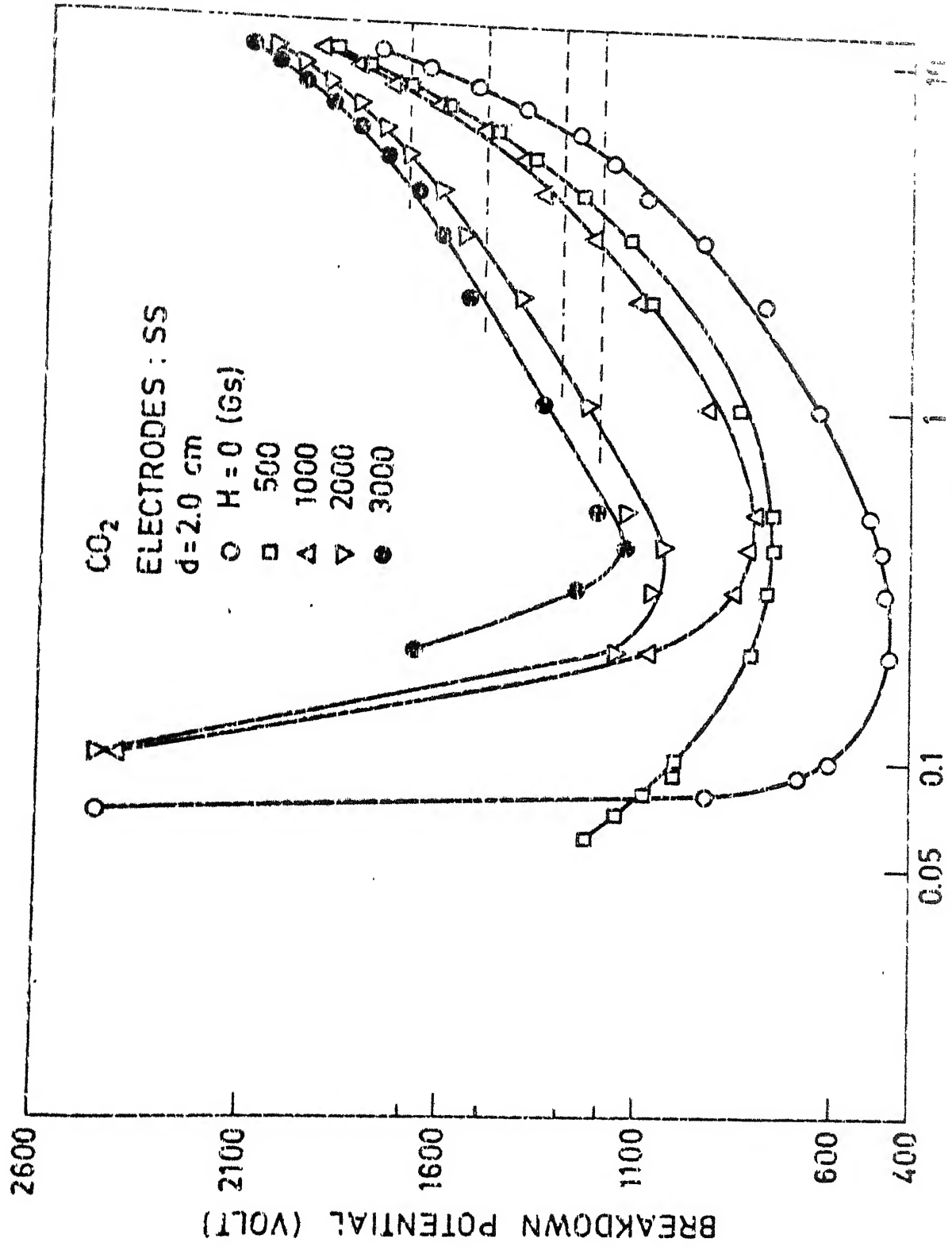

Fig. 17. Sparking voltage characteristics for CO_2, d = 2.0 cm.

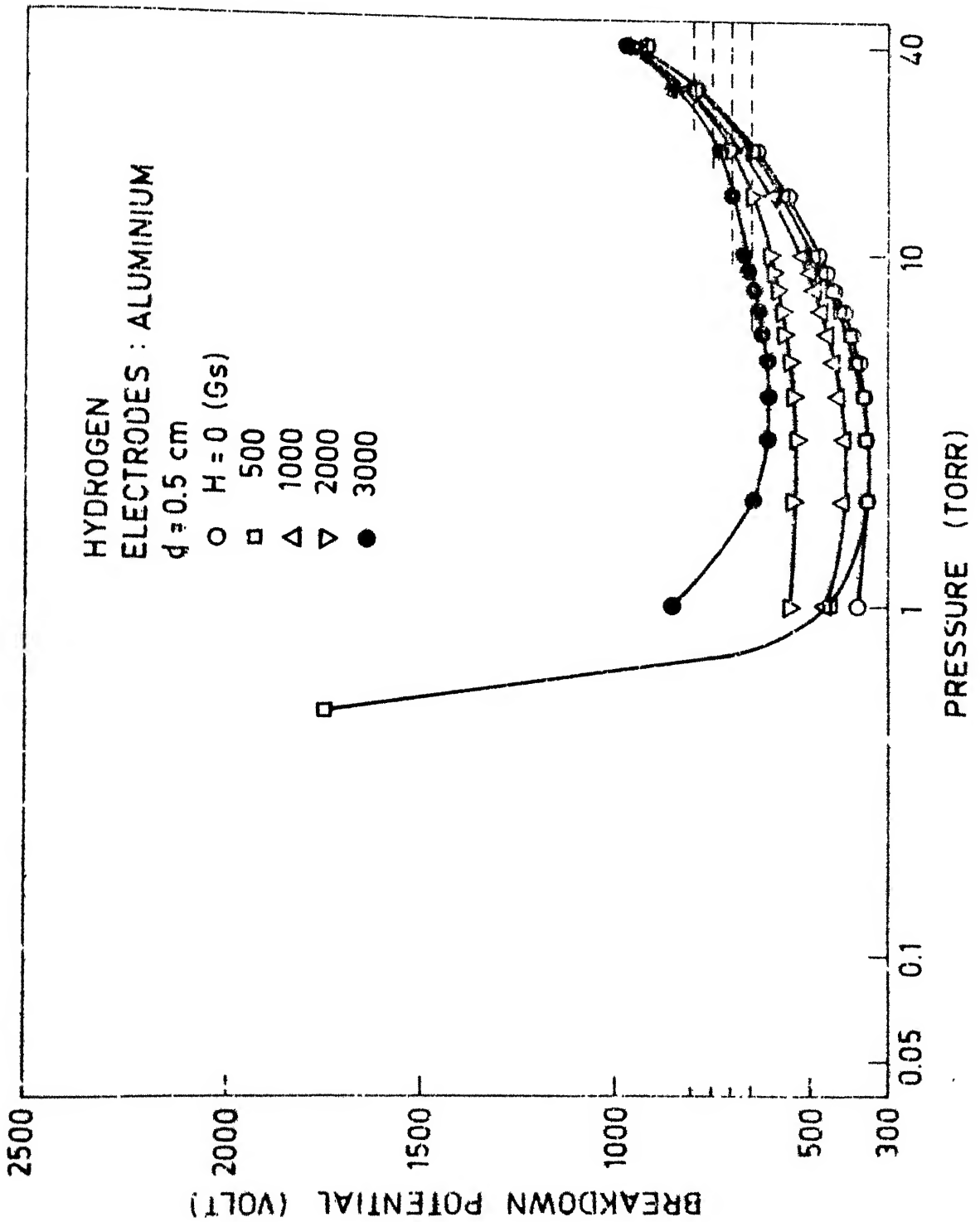

Fig. 18. Sparking voltage characteristics for hydrogen. d = 0.5 cm.

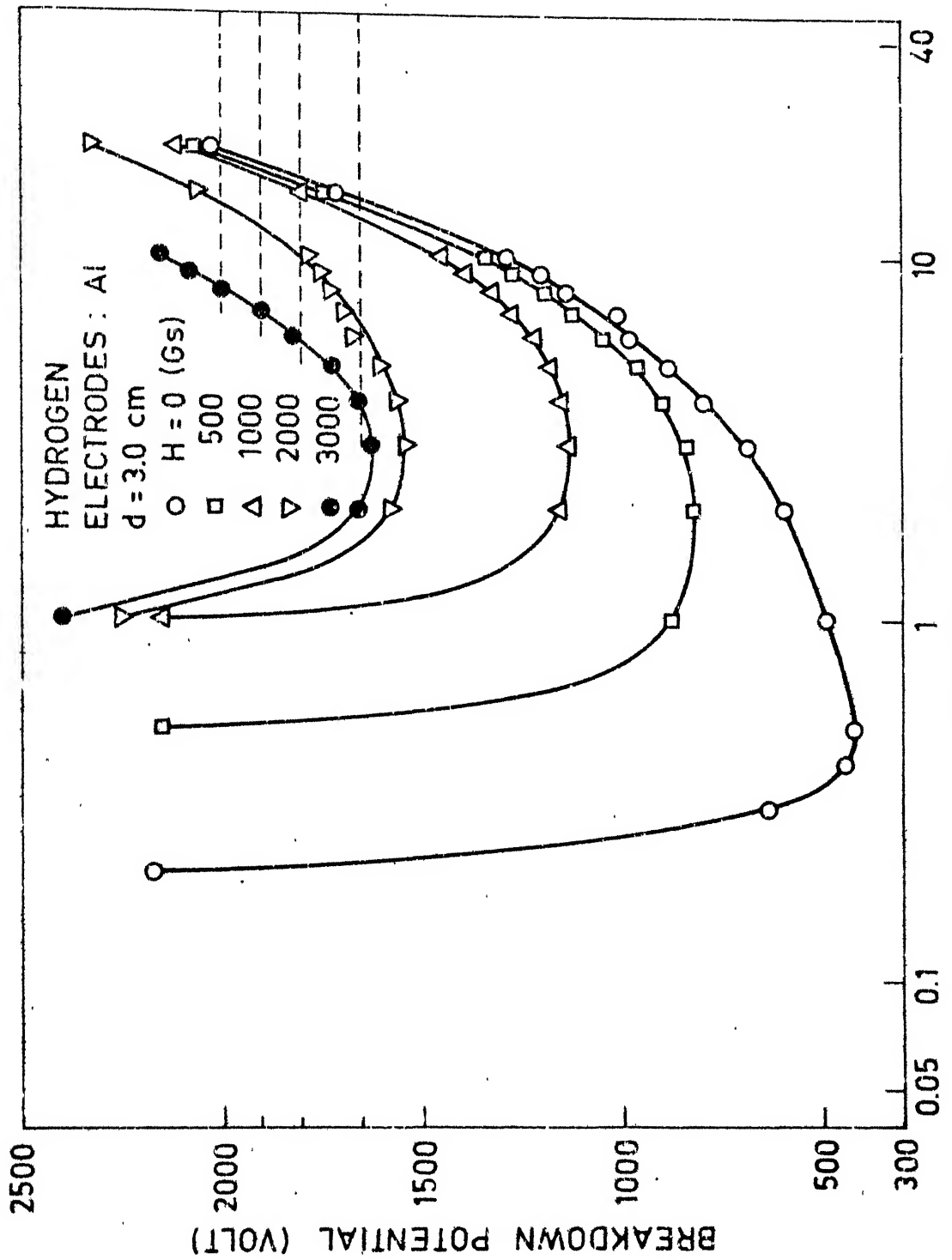

Fig. 19. Sparking voltage characteristics for hydrogen. d = 3.0 cm.

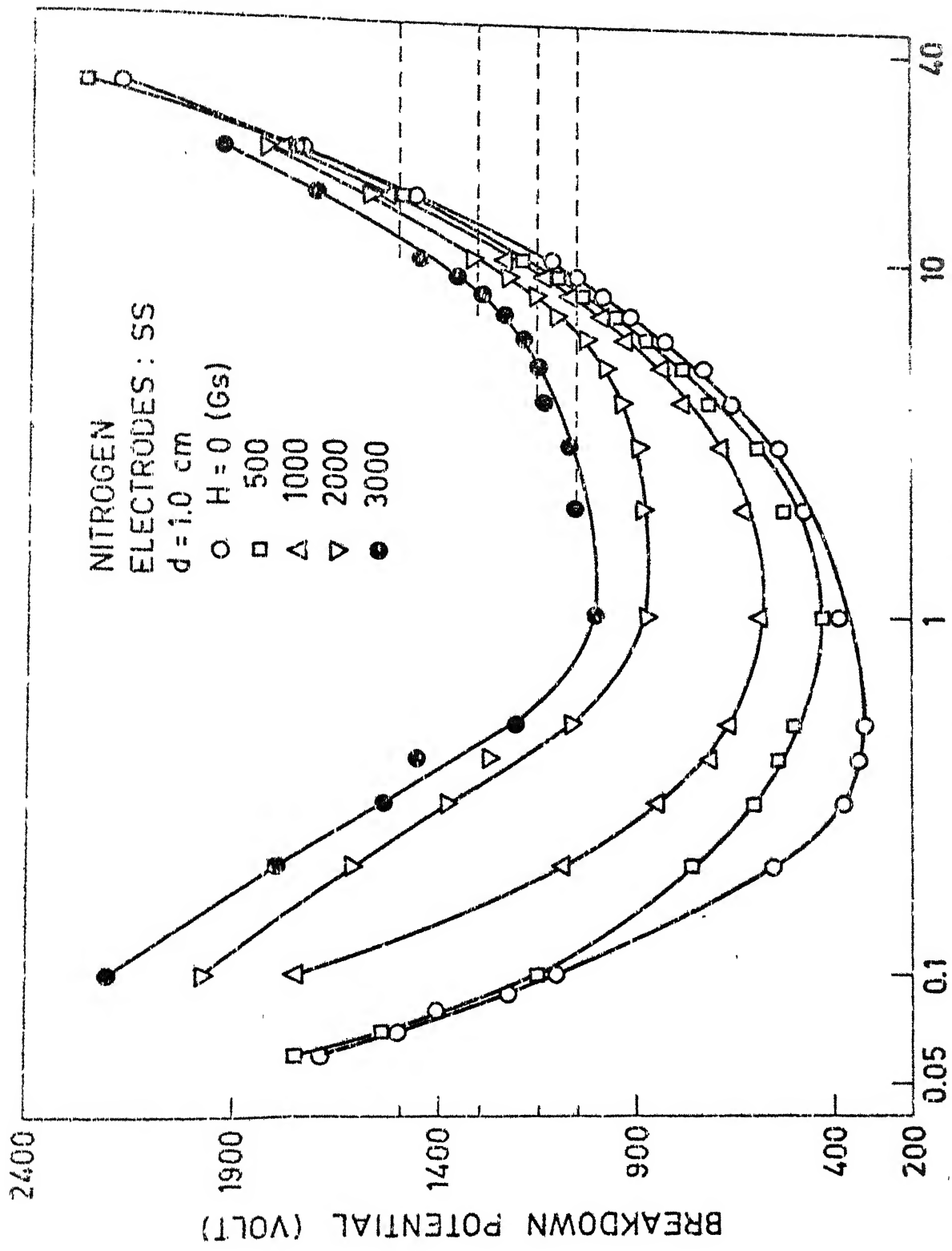

Fig. 20. Sparking voltage characteristics for [illegible]

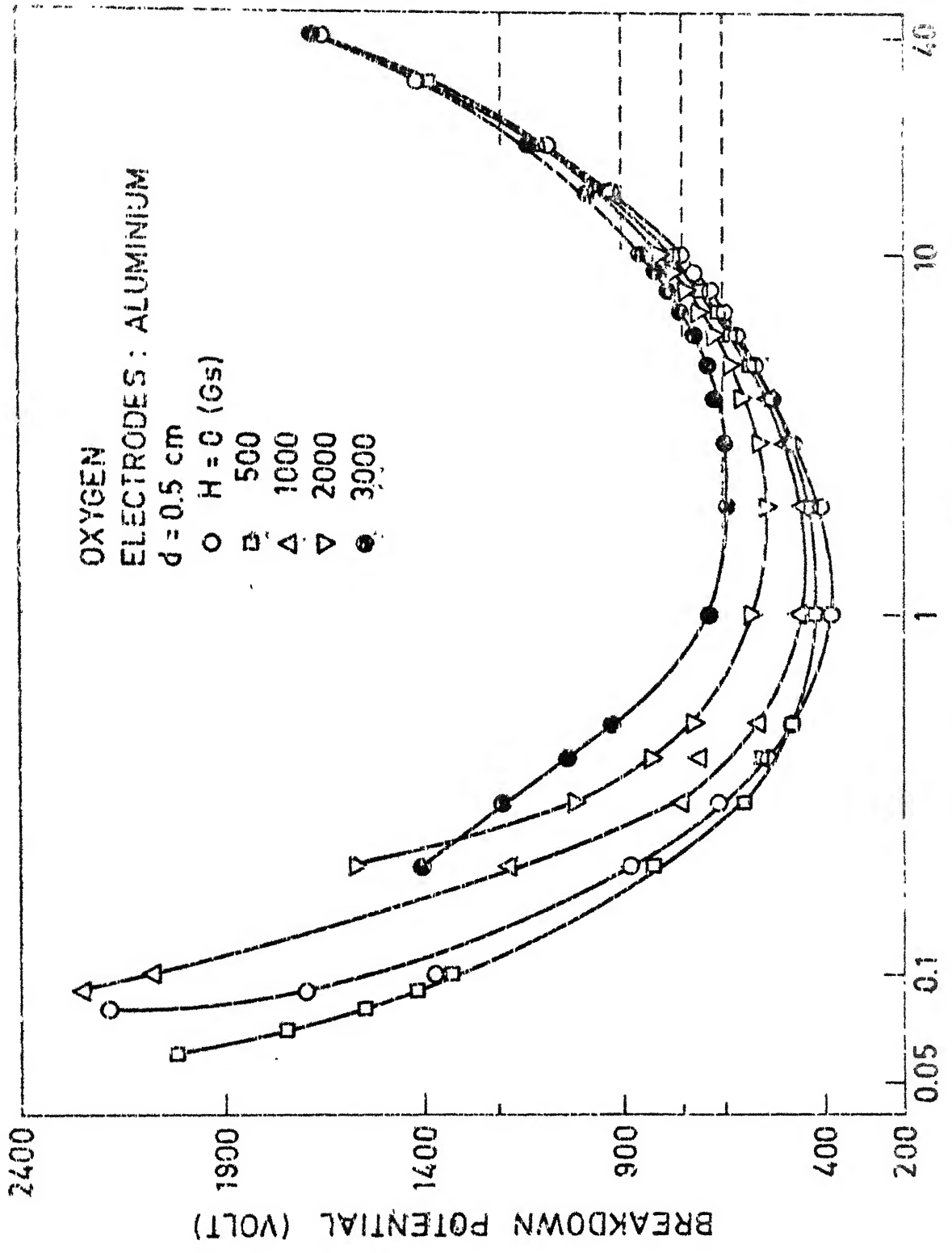

Fig. 21 Sparking voltage characteristics

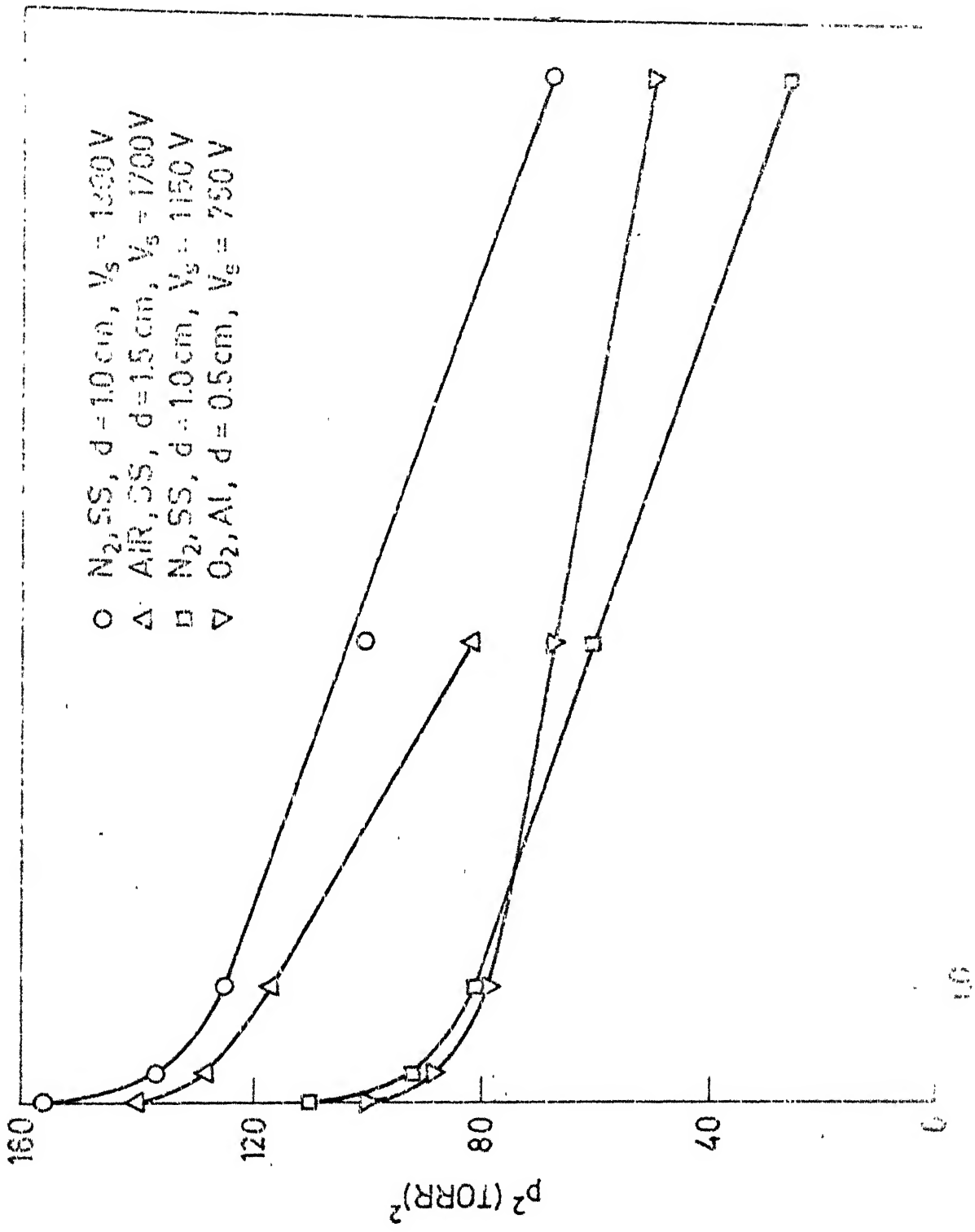
○ N_2, SS, d = 1.0 cm, V_s = 1430 V
△ AIR, SS, d = 1.5 cm, V_s = 1700 V
□ N_2, SS, d = 1.0 cm, V_s = 1150 V
▽ O_2, Al, d = 0.5 cm, V_s = 750 V
160
120
80
40
0
p^2 (TORR)^2

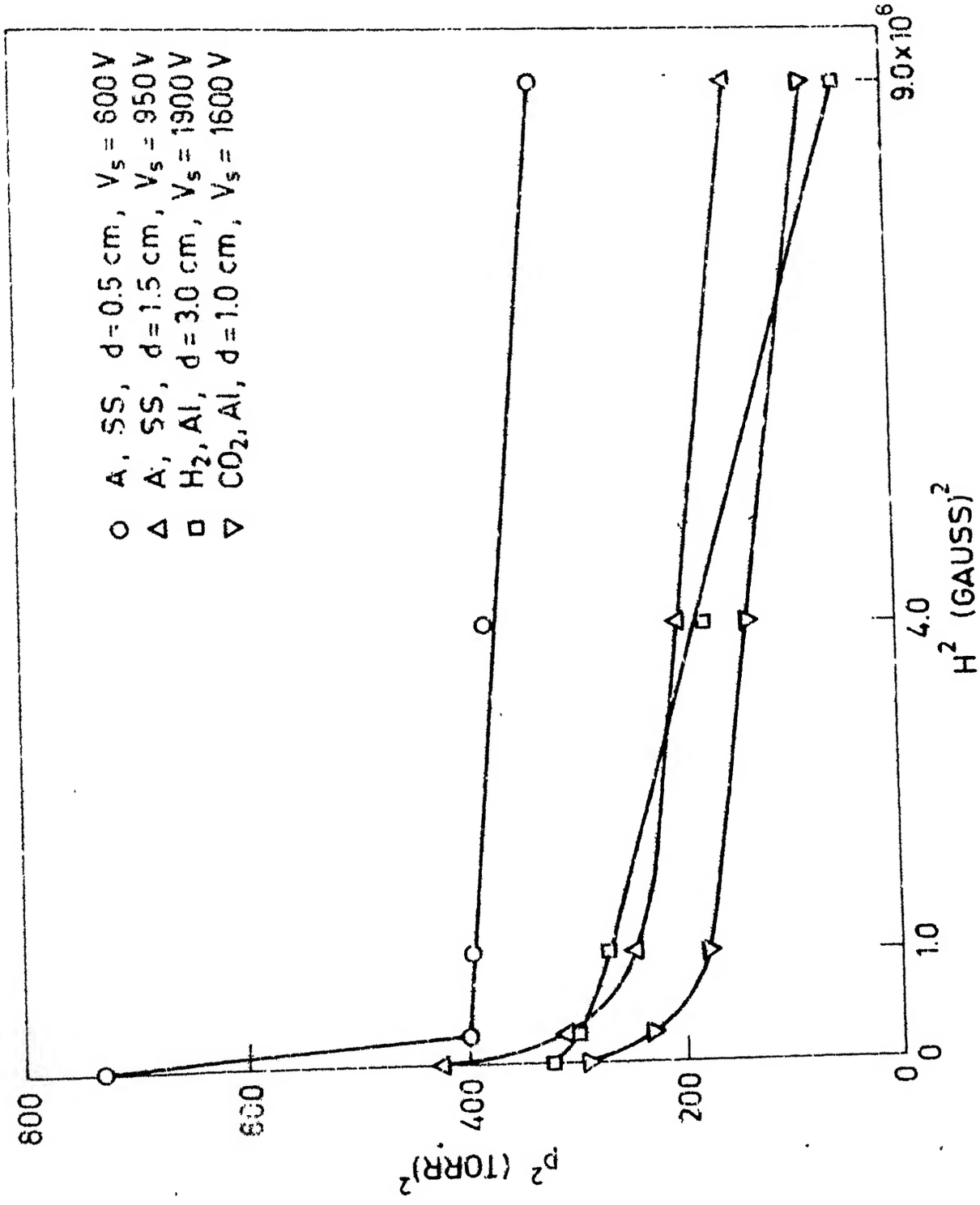

Fig. 23. p^2 vs H^2.

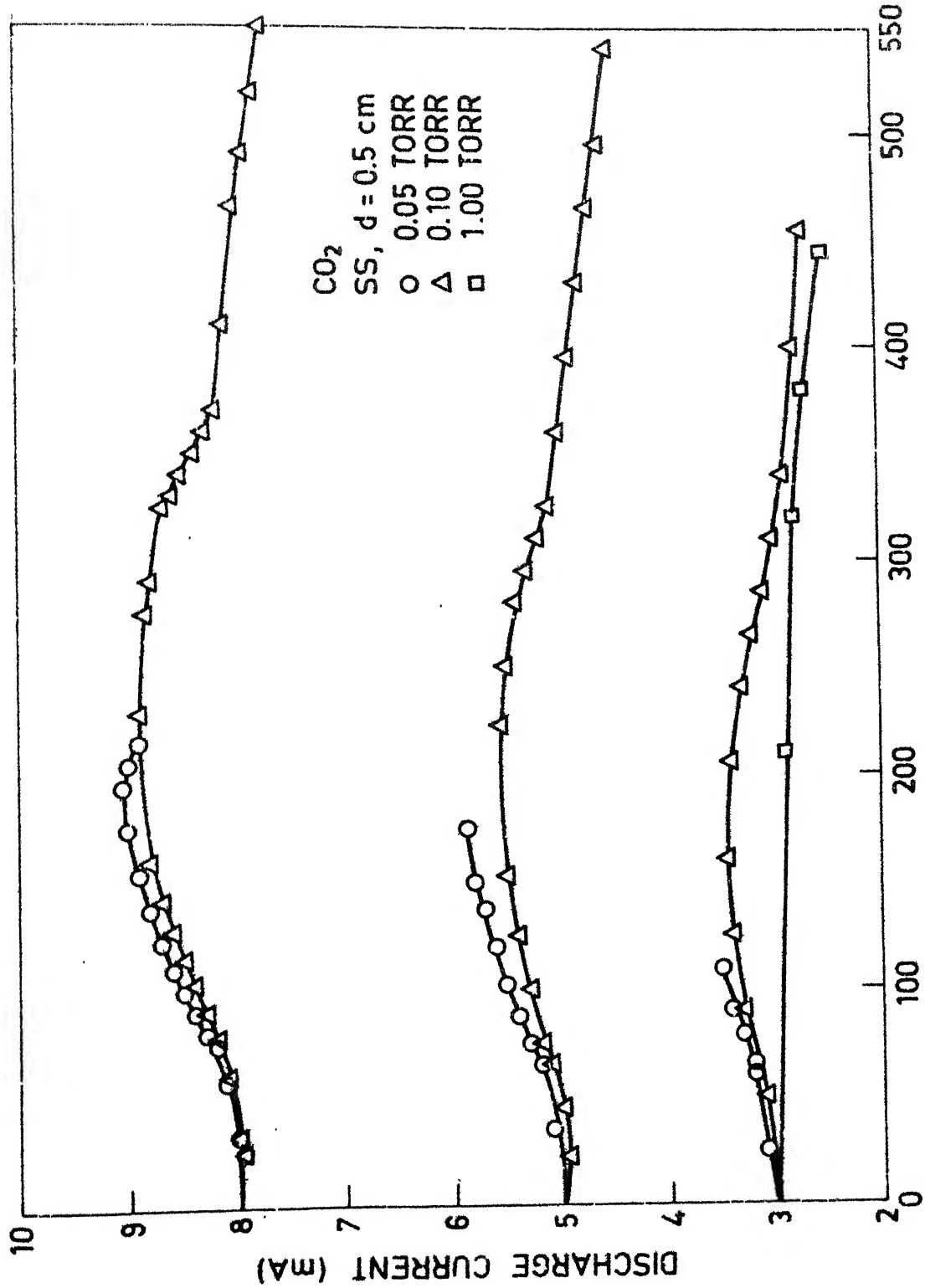

Fig. 24. Influence of transverse magnetic field on discharge current.

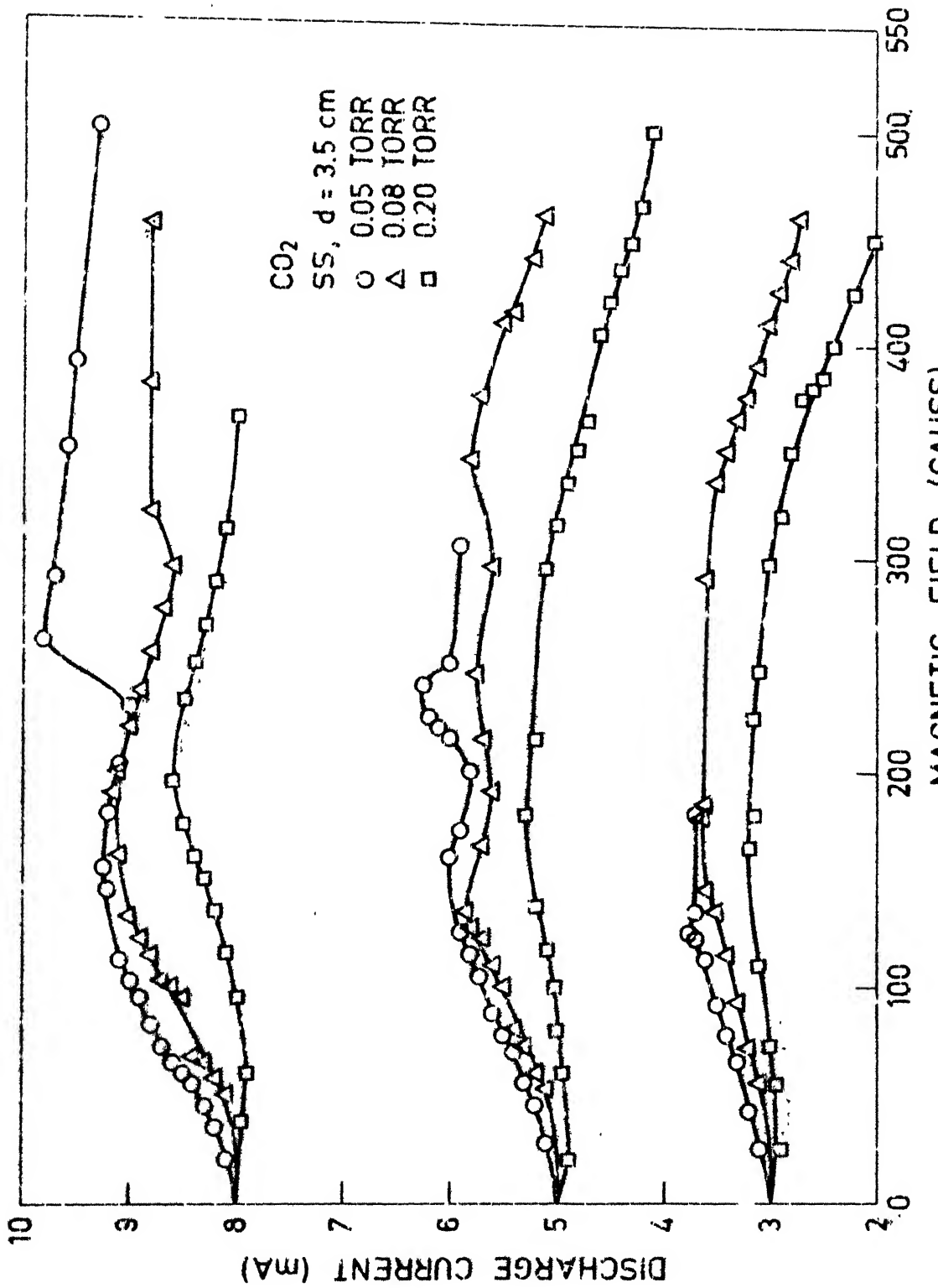

Fig. 25. Influence of transverse magnetic field on discharge current.

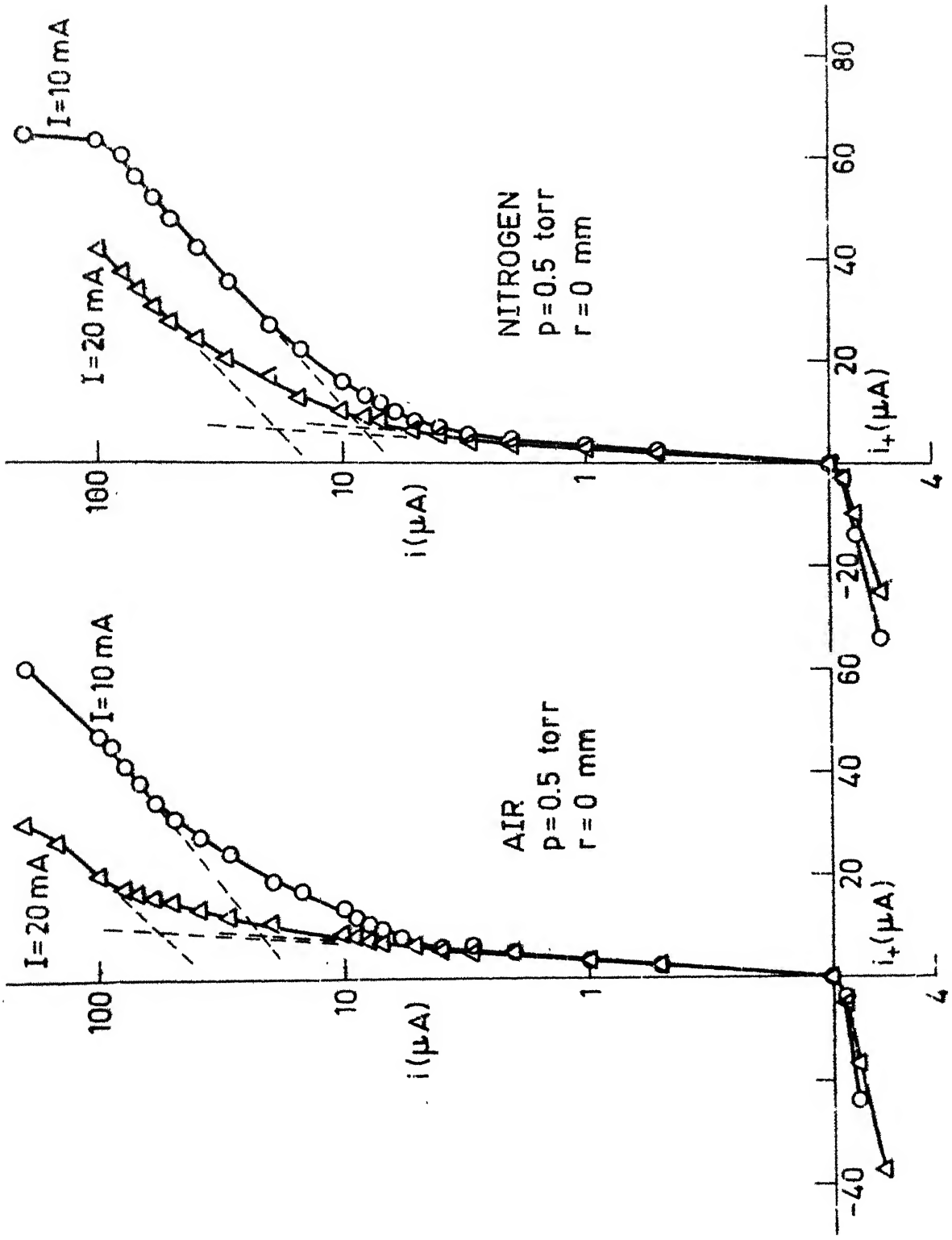

Fig. 26. Probe characteristic in air and nitrogen.

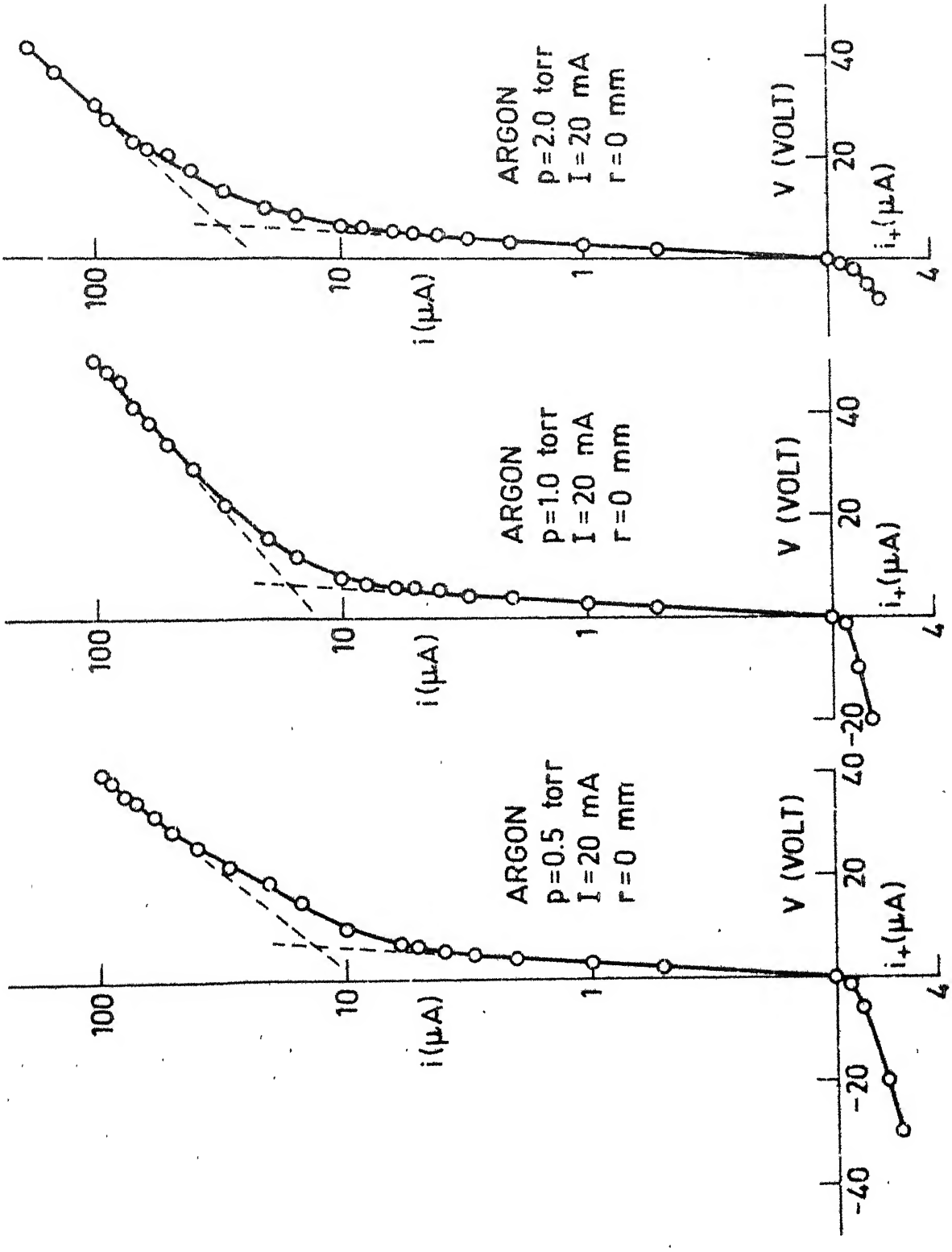

Fig. 27. Probe characteristic in argon.

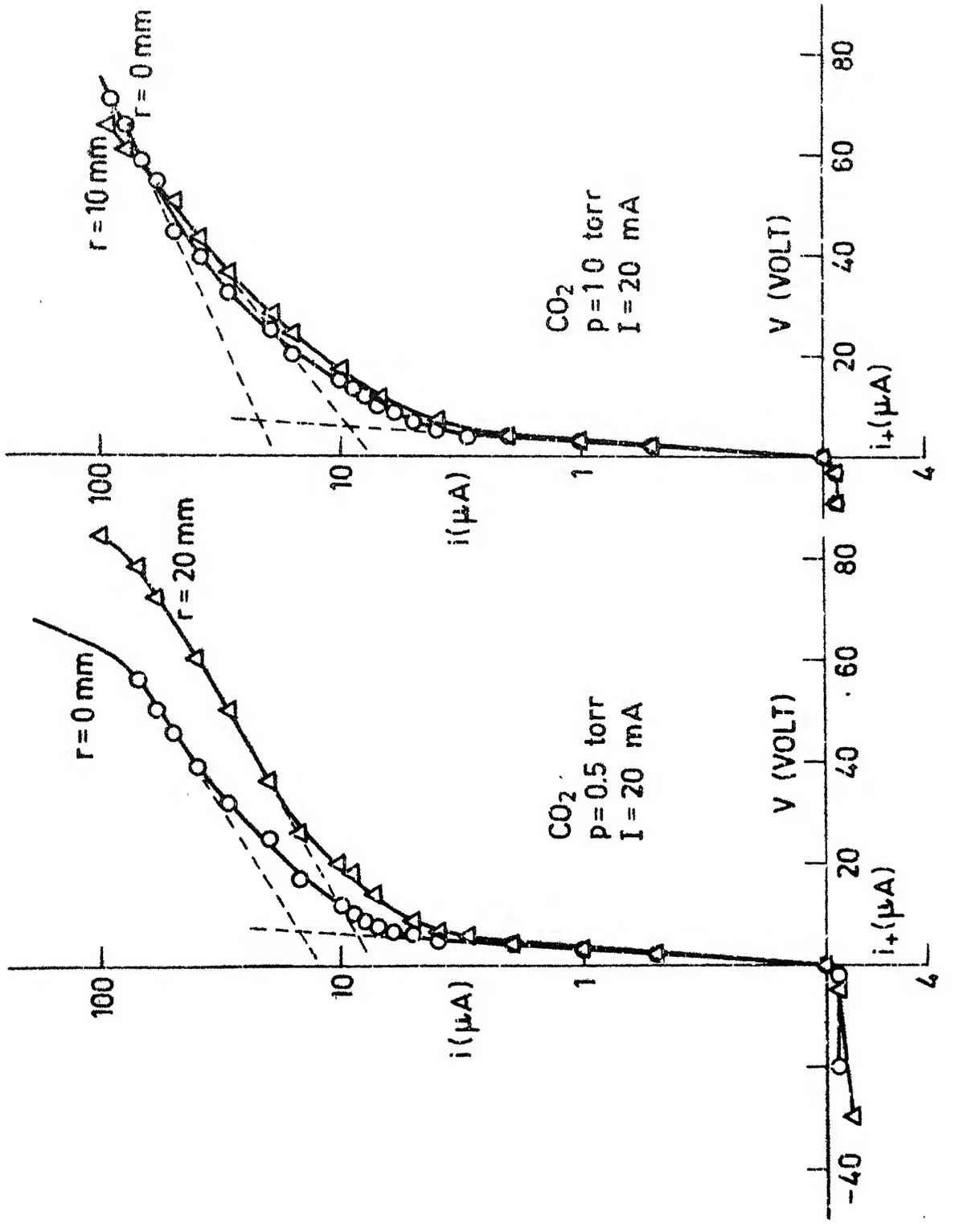

Fig. 28. Probe characteristic in CO_2.

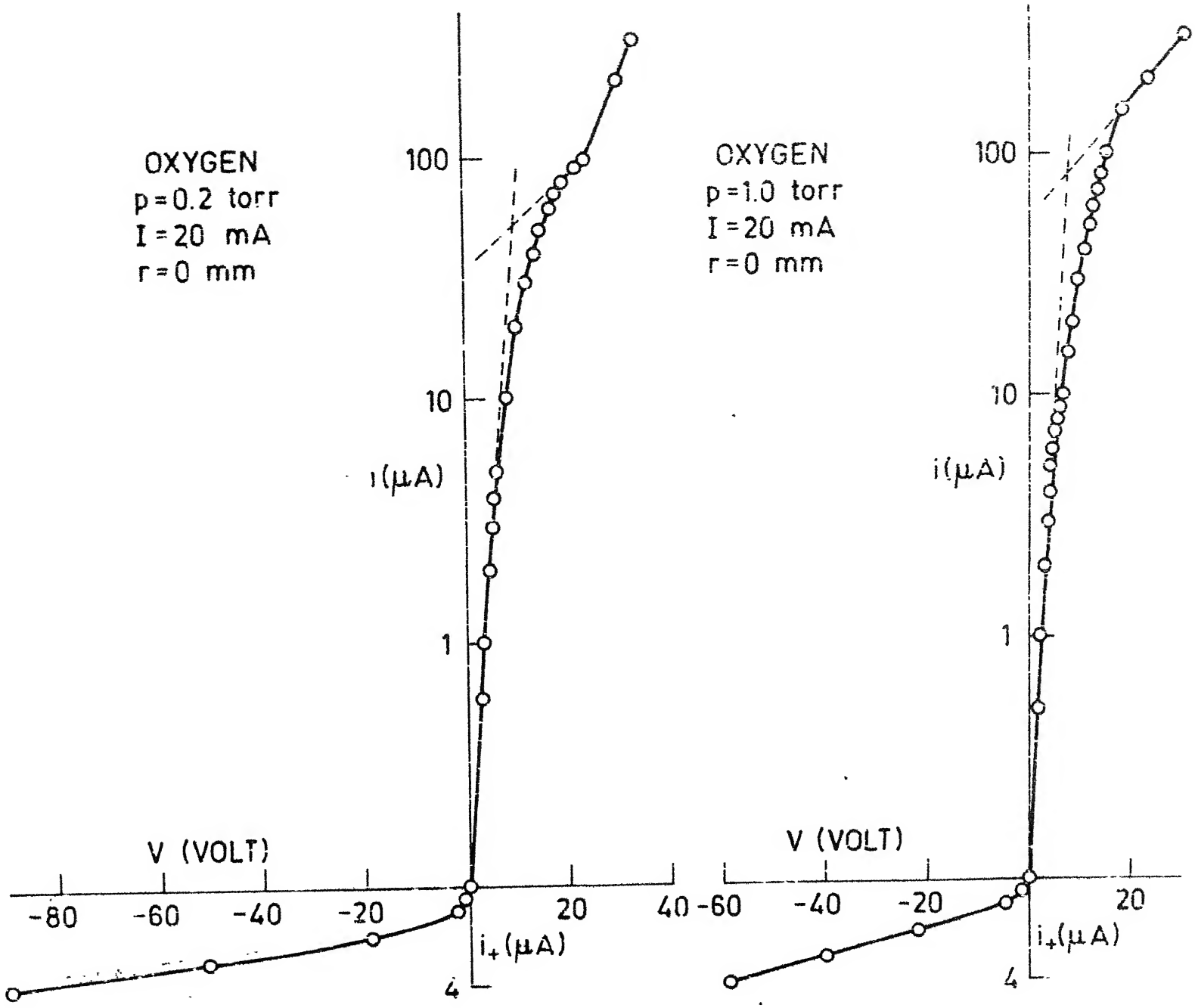

Fig. 29. Probe characteritic in oxygen.